



Acasunlimab, an Fc-inert PD-L1×4-1BB bispecific antibody, combined with PD-1 blockade potentiates antitumor immunity via complementary immune modulatory effects

Michela Capello,¹ Angelica Sette,¹ Theo Plantinga,¹ Craig J Thalhauser,² Vanessa M Spires,² Kristina B Nürmberger,³ Jordan M Blum,² Brandon W Higgs,² Patricia Garrido Castro,¹ Christina Yu,² Carol Costa Sa,² Sina Fellermeier-Kopf,³ Saskia M Burm ,¹ Kristin Strumane ,¹ Aras Toker ,³ Andrea Imle ,³ Bruna de Andrade Pereira,³ Alexander Muik,³ Tahamtan Ahmadi,² Özlem Türeci,³ Mark Fereshteh,² Ugur Sahin,³ Maria Jure-Kunkel,² Nora Pencheva¹

To cite: Capello M, Sette A, Plantinga T, *et al.* Acasunlimab, an Fc-inert PD-L1×4-1BB bispecific antibody, combined with PD-1 blockade potentiates antitumor immunity via complementary immune modulatory effects. *Journal for ImmunoTherapy of Cancer* 2025;13:e011377. doi:10.1136/jitc-2024-011377

► Additional supplemental material is published online only. To view, please visit the journal online (<https://doi.org/10.1136/jitc-2024-011377>).

MC and AS contributed equally.

Accepted 24 March 2025



© Author(s) (or their employer(s)) 2025. Re-use permitted under CC BY-NC. No commercial re-use. See rights and permissions. Published by BMJ Group.

¹Genmab BV, Utrecht, Netherlands

²Genmab US, Plainsboro, New Jersey, USA

³BioNTech SE, Mainz, Rheinland-Pfalz, Germany

Correspondence to

Dr Nora Pencheva; npe@genmab.com

Dr Maria Jure-Kunkel; mjk@genmab.com

ABSTRACT

Background Next-generation cancer immunotherapies aim to improve patient outcomes by combining inhibitory signal blockade with targeted T-cell costimulation in tumor and lymphoid tissues. Acasunlimab (DuoBody-PD-L1×4-1BB) is an investigational, bispecific antibody designed to elicit an antitumor immune response via conditional 4-1BB activation strictly dependent on simultaneous programmed death-ligand 1 (PD-L1) binding. Since 4-1BB is coexpressed with programmed cell death protein-1 (PD-1) on CD8⁺ T cells, PD-1 blockade and simultaneous costimulation through 4-1BB may synergistically enhance T-cell effector functions. We hypothesized that combining acasunlimab with PD-1 blockade to fully disrupt PD-1 interactions with both PD-L1 and PD-L2 would amplify the depth and duration of antitumor immunity.

Methods The effect of acasunlimab and pembrolizumab combination was analyzed in vitro using functional immune cell assays, including mixed-lymphocyte reactions and antigen-specific T-cell proliferation and cytotoxicity assays. The antitumor activity of the combination was tested in vivo in (1) MC38, MB49, Pan02, and B16F10 syngeneic tumor models using acasunlimab and anti-PD-1 mouse-surrogate antibodies; and (2) triple knock-in mice expressing the human targets using an acasunlimab chimeric antibody (chi-acasunlimab) and pembrolizumab. The mechanism of action of the combination was investigated in the MC38 syngeneic model through immunohistochemistry, flow cytometry, and bulk RNA sequencing.

Results The combination reinvigorated dysfunctional T cells in vitro, while also potentiating T-cell expansion, interleukin (IL)-4 and interferon gamma secretion and cytotoxic activity. In vivo, the combination of chi-acasunlimab and pembrolizumab or mouse-surrogate antibodies potentiated antitumor activity and survival in the humanized knock-in and multiple syngeneic mouse models, leading to durable complete tumor regressions in the MC38 model consistent with therapeutic synergy.

WHAT IS ALREADY KNOWN ON THIS TOPIC

⇒ Combining programmed cell death protein-1 (PD-1)/programmed death-ligand 1 (PD-L1) blockade with 4-1BB agonism has shown promise in reinvigorating antitumor T-cell responses in preclinical models. The novel combination therapy of acasunlimab (DuoBody-PD-L1×4-1BB), an investigational PD-L1 and 4-1BB-targeting bispecific antibody, with pembrolizumab has recently demonstrated promising clinical activity in checkpoint inhibitor (CPI)-relapsed/refractory metastatic non-small cell lung cancer (NSCLC). This study investigated the mechanisms of antitumor immunity conferred by this combination therapy.

WHAT THIS STUDY ADDS

⇒ This study offers key mechanistic insights into the complementary immune modulatory effects of acasunlimab-mediated conditional T-cell costimulation through 4-1BB combined with full PD-1 blockade. The combination amplifies the depth and duration of antitumor immune responses by promoting autocrine interleukin 2–CD25 signaling and inducing stem-like CD8⁺ tumor-infiltrating T cells with enhanced effector functions.

Mechanistically, the combination enhanced clonal expansion of tumor-specific CD8⁺ T cells in tumor-draining lymph nodes and increased the density of proliferating and cytotoxic CD8⁺ T cells in the tumor microenvironment. It also potentiated the IL-2 signaling pathway, increasing the proportion of granzyme B (GZMB⁺) stem-like CD8⁺ T cells thought to have superior effector function.

Conclusion These preclinical results demonstrate that conditional 4-1BB stimulation combined with complete PD-1 blockade enhances antitumor immunity through complementary mechanisms. The acasunlimab

HOW THIS STUDY MIGHT AFFECT RESEARCH, PRACTICE OR POLICY

⇒ These findings provide a robust mechanistic rationale for combining targeted 4-1BB costimulation in tumor and lymphoid tissues with full PD-1 blockade to amplify adaptive antitumor immunity, establishing the preclinical foundation for the clinical development of acasunlimab in combination with pembrolizumab. This combination approach is currently being evaluated in a pivotal Phase 3 study (ABBILITY NSCLC-06; NCT06635824) for patients with metastatic NSCLC who have failed prior CPI therapy.

and pembrolizumab combination is being evaluated in Phase 2 (NCT05117242) and pivotal Phase 3 (NCT06635824) trials in patients with metastatic non-small cell lung cancer after checkpoint inhibitor therapy failure.

BACKGROUND

Programmed cell death protein-1 (PD-1)/programmed death-ligand 1 (PD-L1) checkpoint inhibitors (CPIs) have transformed the treatment paradigm and prognosis for several advanced solid tumor indications.¹ However, clinical efficacy to CPI-containing therapy is observed only in a subset of patients, with the majority progressing after an initial response. This underscores the need for better patient selection strategies and combination therapies to improve patient outcomes. The combination of immune CPIs targeting complementary pathways has demonstrated improved antitumor activity compared with single-agent CPIs in the clinic.² To unleash the full potential of adaptive immunity, it may be beneficial to combine blockade of inhibitory signals with simultaneous activation of costimulatory receptors to promote T-cell proliferation, survival, and effector functions, and to reinvigorate T cells that became exhausted and dysfunctional due to sustained antigen stimulation in the tumor microenvironment (TME).^{3–7} One such costimulatory receptor is 4-1BB that can induce expansion of T-cell clones, enhance memory differentiation, and improve functionality and survival of dysfunctional CD8⁺ T cells in the TME.^{8–10} 4-1BB is a clinically validated target, with agonistic 4-1BB monospecific antibodies demonstrating promising initial biological activity, however with a limited therapeutic window due to dose-limiting hepatotoxicity.^{9, 11} Therefore, next-generation 4-1BB agonists aim to broaden the therapeutic window by restricting 4-1BB activation to tumor and lymphoid tissues in a manner strictly dependent on cotargeting complementary immune checkpoint pathways.⁹

The potential for concurrent targeting of 4-1BB and PD-1 is supported by their coexpression on antigen-specific CD8⁺ T cells during different states of activation, including activated, memory and (pre)exhausted CD8⁺ T cells in the TME.^{5, 12–16} Preclinical studies have shown that the combination of PD-1/PD-L1 (PD-(L)1)-blocking agents and 4-1BB agonists can reinvigorate the function of exhausted CD8⁺ tumor-infiltrating

lymphocytes (TILs) and exert synergistic antitumor effects associated with potent tumor antigen-specific T-cell responses.^{14, 17–20}

PD-L1 and 4-1BB targeting bispecific antibodies, which combine conditional 4-1BB agonist activity with PD-(L)1 checkpoint blockade, have shown promise in enhancing antitumor activity, while allowing for an improved safety profile over earlier generation 4-1BB monoclonal antibodies.^{21–27} Acasunlimab (GEN1046/BNT311/DuoBody-PD-L1×4-1BB) is a PD-L1×4-1BB bispecific antibody that is in clinical development for the treatment of patients with solid tumors (NCT03917381, NCT04937153, NCT05117242, and NCT06635824). Due to its innovative design using the clinically validated DuoBody platform for the generation of bispecific antibodies in combination with an inert fragment crystallizable (Fc) region, the 4-1BB agonist activity of acasunlimab is strictly dependent on binding to PD-L1⁺ tumor cells and/or PD-L1⁺ immune cells, thus predominantly limiting the immune response to the site of the tumor and secondary lymphoid organs. At the same time, the PD-L1-specific arm of acasunlimab functions as a classical immune CPI by blocking the PD-1/PD-L1 axis irrespective of 4-1BB binding. Acasunlimab was shown to exert superior T-cell activation and T-cell-mediated cytotoxicity compared with clinically approved PD-L1 antibodies *in vitro*, and to promote expansion of tumor-reactive TILs *ex vivo*.²⁵ In preclinical mouse tumor models, acasunlimab exerted potent antitumor activity, which was associated with enhanced intratumoral CD8⁺ T-cell infiltration.²⁵ In the clinic, single-agent acasunlimab has shown a manageable safety profile and early clinical activity in heavily pretreated patients with advanced solid tumors, including patients who had progressed on prior CPI-containing therapy.²⁵

Pharmacokinetic (PK)/pharmacodynamic modeling using clinical data from the dose escalation phase of the first-in-human study indicated that doses of acasunlimab achieving optimal 4-1BB activation result in partial PD-1/PD-L1 axis blockade.²⁸ This suggests that blockade of the PD-1 pathway could be enhanced by combining acasunlimab with an anti-PD-1-blocking antibody, allowing for concurrent optimum 4-1BB stimulation and complete inhibition of the PD-1 pathway by fully disrupting its interactions with both PD-L1 and PD-L2.

In this study, we provide preclinical evidence that combining acasunlimab-induced conditional 4-1BB costimulation with complete blockade of the PD-1 pathway leads to improved depth and duration of the antitumor immune response through distinct and complementary immune modulatory effects.

METHODS

Antibodies, cancer cell lines and reagents

Details on antibodies, cancer cell lines, and buffers are listed in the online supplemental materials and methods.

Human primary leukocytes

Details on the preparation of human primary lymphocytes and dendritic cells (DCs) used in the *in vitro* T-cell assays are described in the online supplemental materials and methods. Briefly, CD14⁺ monocytes were obtained from human healthy donor peripheral blood mononuclear cells (PBMCs) and differentiated into immature DCs (iDCs) using granulocyte macrophage-colony stimulating factor (BioLegend, 766106) and interleukin (IL)-4 (BioLegend, 766206), and then lipopolysaccharide-matured to mature DCs (mDCs). For the antigen-specific T-cell assays, PBMC-derived CD8⁺ T cells were electroporated to express a human Claudin-6 (CLDN6)-specific mouse T-cell receptor (TCR) and human PD-1, and iDCs were electroporated to express human CLDN6.

In vitro studies

Mixed lymphocyte reaction with functional T cells

In the mixed lymphocyte reaction (MLR) assay (online supplemental figure 1A), purified CD8⁺ T cells were thawed and resuspended at 1×10^6 cells/mL in Roswell Park Memorial Institute (RPMI) 1640 complete medium (Thermo Fisher Scientific, A1049101) supplemented with 10% fetal bovine serum (FBS; Gibco, 16140071) and 10 ng/mL IL-2 (BioLegend, 589106) at 37°C O/N. CD8⁺ T cells were then co-cultured with allogeneic mDCs in 96-well plates (1:10 mDC:T-cell ratio) and incubated with a dose range of acasunlimab, including clinically relevant concentrations,^{25 28} either alone or combined with pembrolizumab, or with control antibodies in MLR assay medium at 37°C for 5 days. Single-agent pembrolizumab samples were tested with an antibody dose range, whereas in combination with the acasunlimab dose range, 1 µg/mL pembrolizumab was tested, which was previously determined as the maximal-effective concentration in this assay. Supernatants were harvested for cytokine analysis.

MLR with dysfunctional T cells

Dysfunctional T cells (T_{dys}) were prepared by stimulating 1×10^6 cells/mL purified healthy donor CD3⁺ T cells twice with anti-CD3/CD28 Dynabeads (Gibco, 11161D) (1:1 bead-to-cell ratio) in MLR assay medium supplemented with 5% FBS and 10 ng/mL IL-2 at 37°C for a total of 120 hours (after an initial 72 hours, the beads were removed and fresh anti-CD3/CD28 beads were added for an additional 48 hours). The dysfunctional phenotype of the T cells was confirmed as described in the online supplemental materials and methods (online supplemental figure 2A–D). Dysfunctional CD3⁺ T cells were rested for 24 hours in RPMI 1640 medium supplemented with 10% FBS and 10 ng/mL IL-2 before co-culturing with allogeneic mDCs in 96-well plates (1:4 or 1:10 DC:T-cell ratio) and incubating with a dose range of acasunlimab, either alone or combined with 0.8 µg/mL pembrolizumab (previously determined as the maximal-effective concentration in this assay), or with control antibodies in MLR assay medium at 37°C for 5 days. Supernatants were harvested for cytokine analysis.

Antigen-specific T-cell proliferation assay

Electroporated human CD8⁺ T cells expressing the CLDN6-TCR and human PD-1 were labeled with carboxy-fluorescein succinimidyl ester (CFSE) using the Vybrant CFDA SE Cell Tracer Kit (Life Technologies, V12883). 75,000 CFSE-labeled T cells were co-cultured with 7,500 autologous iDCs electroporated to express human CLDN6 (1:10 DC:T-cell ratio) in 96-well plates and incubated with a dose range of acasunlimab, either alone or combined with 0.8 µg/mL pembrolizumab (previously determined as the maximal-effective concentration in this assay), or with control antibodies in T-cell proliferation assay medium at 37°C for 4 days. CD8⁺ T-cell proliferation was calculated from CFSE dilution measured by flow cytometry. Generation peaks were automatically fitted using the proliferation modeling tool in FlowJo and used to calculate expansion index values. Supernatants were harvested for cytokine analysis (online supplemental figure 1B).

Antigen-specific T-cell-mediated cytotoxicity assay

MDA-MB-231_hCLDN6 cells, which endogenously express human PD-L1, were seeded (1.5×10^4 cells/well) in xCELLigence E-plates (Agilent, 05232368001) 1 day before adding electroporated CD8⁺ T cells expressing a CLDN6-TCR and human PD-1 at an effector to target cell (E:T) ratio of 3:1. The co-cultures of tumor cells and CD8⁺ T cells were incubated with acasunlimab fixed concentrations of 0.003 µg/mL (ie, predetermined EC₂₀) or 0.0015 µg/mL (ie, <EC₂₀), either alone or with 0.8 µg/mL pembrolizumab (predetermined maximal-effective concentration), or with control antibodies. Cells in the E-plates were cultured in the xCELLigence real-time cell analysis instrument (ACEA Biosciences) for 140–170 hours without disturbance, with impedance measurements at 2-hour intervals. Impedance measurement data were normalized to the time of co-culture start for each treatment condition and data were expressed relative to T cell-tumor cell co-cultures without antibody (set to 100%). Pooled real-time cell analysis over the assay period was performed using GraphPad Prism's area under the curve (AUC) function (online supplemental figure 1C). Expression of CD107a and GZMB by the CD8⁺ T cells was also assessed as described in the online supplemental materials and methods.

In vivo studies

PK analysis of anti-mPD-L1×m4-1BB and mouse mPBPK/RO modeling

MC38 tumor-bearing mice were treated with 5 or 20 mg/kg anti-mouse PD-L1 × anti-mouse 4-1BB (anti-mPD-L1×m4-1BB) antibody twice weekly for three weeks (Q2W×3) as single agent or in combination with 10 mg/kg anti-mouse PD-1 (anti-mPD-1) antibody clone RMP1-14 (three mice per group) and blood samples were collected for PK analysis as described in the online supplemental materials and methods. A minimal physiologically-based PK model with receptor occupancy (mPBPK/RO) was developed by supplementing a published mPBPK model

with a tumor compartment.²⁹ Tumor distribution of the antibody was taken as previously described.³⁰ T cells could interact with nearby tumor cells via both mPD-L1 on the tumor cells engaging mPD-1 on the T-cell membrane and via anti-mPD-L1×m4-1BB engagement of m4-1BB on the T cells and mPD-L1 on the tumor cells. Cells in the model were assumed to be static; no growth or death was considered, only the formation of complexes on their membranes. PK parameters (clearance and distribution rates) were estimated from data of anti-mPD-L1×m4-1BB (online supplemental figure 3) and anti-mPD-1.³¹ A typical tumor volume of 50 mm³ was used to initialize the model. T-cell infiltration and 4-1BB expression at baseline were taken from immunohistochemistry (IHC) analysis of phosphate-buffered saline (PBS)-treated control animals on day 7 under the assumption that the relative proportion would not change in these control animals between the start of treatment and day 7.

In vivo efficacy study in C57BL/6 mice implanted with B16F10, MB49, MC38 and Pan02 tumors

C57BL/6 mice were purchased from Vital River Laboratories Research Models and Services (Beijing, China) or GemPharmatech. Mice were subcutaneously (SC) injected in the right flank with B16F10 (2×10⁵ cells/mouse), MB49 (1×10⁶ cells/mouse), MC38 (1×10⁶ cells/mouse), or Pan02 (3×10⁶ cells/mouse) in 100 µL PBS. At randomization of the animals into treatment groups, the mean tumor volumes reached 39 mm³ for B16F10, 59 mm³ for MB49, 60 mm³ for MC38, and 90 mm³ for Pan02. Tumor-bearing mice were treated by repeated intraperitoneal (IP) injections twice weekly for three weeks (2QW×3) of 10 mg/kg anti-mPD-1 antibody clone RMP1-14, 5 mg/kg anti-mPD-L1×m4-1BB, the combination thereof, or with PBS (10 mice per group). Animals implanted with MC38 tumor cells that achieved complete tumor regression (CR) after treatment were rechallenged by SC injection of MC38 tumor cells on day 138 after the initial start of treatment. As a control group for the rechallenge analysis, a second cohort of treatment-naïve animals was inoculated with MC38 tumor cells.

In vivo efficacy study in hPD-1/hPD-L1/h4-1BB tKI mice implanted with MC38-hPD-L1 and MC38 tumors

C57BL/6-*Pdcd1*^{tm1(PDCD1)*Bcgen*} *Cd274*^{tm1(CD274)*Bcgen*} *Tnfrsf9*^{tm1(TNFRSF9)*Bcgen*} /*Bcgen* mice engineered to express extracellular domains of human PD-1, PD-L1 and 4-1BB in the mouse PD-1, PD-L1 and 4-1BB gene loci (hPD-1/hPD-L1/h4-1BB) triple knock-in (tKI) mice were purchased from Beijing Biocytogen (130569). In this model, chimeric acasunlimab (chi-acasunlimab) was tested, which is a chimeric antibody containing the V_H/V_L sequences of acasunlimab in a mouse IgG2a backbone with Fc-inertness mutations. The experimental set-up was based on previous experience²⁵ and dose optimization studies (data not shown). Mice were SC injected in the right flank with 1×10⁶ MC38-hPD-L1 or wild type (WT) MC38 cells in 100 µL PBS. At randomization of the animals into

treatment groups, the mean tumor volumes reached 128 mm³ for MC38-hPD-L1 and 61 mm³ for MC38. Tumor-bearing mice were treated 2QW×3 by IP injections with chi-acasunlimab (5 mg/kg or 10 mg/kg), pembrolizumab (10 mg/kg), the combination thereof, or matched isotype control antibodies mIgG2a-ctrl and IgG4 (eight mice per group). In the MC38-hPD-L1 tumor model, animals with CR after treatment were rechallenged by SC injection of 1×10⁶ MC38-hPD-L1 tumor cells in the left flank on day 143 after the initial start of treatment. As a control group for the rechallenge analysis, a second cohort of treatment-naïve animals was inoculated with MC38-hPD-L1 tumor cells.

In vivo MoA studies using plasma and tissues from MC38 tumor-bearing C57BL/6 mice

For the in vivo mechanism of action (MoA) studies, C57BL/6 mice were injected with MC38 cells and treated as described for the efficacy study with the only difference that a 2QW dosing frequency was used. On day 7 and day 14 after the start of treatment, mice were euthanized and tumor tissue and/or tumor-draining lymph nodes (tdLNs) were collected for IHC, flow cytometry, TCR sequencing, and RNA sequencing as described in the online supplemental materials and methods.

Statistical analyses

In vitro studies

For the MLR and antigen-specific T-cell proliferation assays, adjusted p values for single-agent activity were calculated using one-way analysis of variance with Dunnett's multiple comparisons test and Highest Single Agent (HSA) synergy analysis was performed using the SynergyFinder R package.³² For HSA synergy analysis, data were processed for each donor or donor pair separately and the measured value of each sample was normalized by subtracting the control values (no treatment control wells) and expressed as a percentage of the maximal value in the assay. Synergy was defined as the excess over the maximum single-agent response based on the HSA model stating that the expected combination effect equals the higher effect of individual drugs. HSA scores >10 are suggestive of synergy. Statistical analyses of the in vitro cytotoxicity studies were performed using a non-parametric, paired Friedman test with Dunn's multiple comparisons test on percentages of CD107a⁺/GZMB⁺ cells or the AUC of normalized real-time analysis data.

In vivo studies

For the in vivo studies in mouse models, tumor growth rate was determined by performing a simple linear regression of the log-transformed tumor volumes. Kaplan-Meier curves of progression-free survival (PFS), defined as mice with tumor volumes <1000 mm³ for B16F10 and MB49, and <500 mm³ for MC38 and Pan02, were analyzed using Mantel-Cox analyses in SPSS. Therapeutic synergy in the in vivo efficacy studies was defined as an antitumor effect

in which the combination of agents demonstrated significant superiority ($p < 0.05$) relative to the activity shown by each agent alone.³³ For IHC, flow cytometry, and cytokine readouts, differences between treatment groups were analyzed using Mann-Whitney or Kruskal-Wallis analysis in GraphPad Prism. Only significant differences ($p < 0.05$) between treatment groups are indicated in the presented figures. Differences were classified as a trend when $0.05 \leq p < 0.1$. All reported p values are two-sided.

TCRseq data analysis

For TCRseq data analysis, clonal diversity was calculated using the generalized diversity index (Hill numbers) over a range of diversity orders (q) to generate a smooth curve with the alphaDiversity function from the alakazam R package in the Immcan-tation framework. Pairwise statistical significance between groups was assessed by constructing a bootstrap delta distribution across groups with 100 realizations. Clonal abundance distribution between treatment groups and tissue compartments (tumor and tLNs) was estimated using the estimateAbundance function from the Alakazam R package with 100 bootstrap realizations to derive 95% CIs.

RNAseq data analysis

For RNAseq data analysis, differential gene expression between treatment groups was calculated in R V.4.4.1 with a Welch's modified t -test. Differentially expressed transcripts with a p value < 0.01 and fold change > 2 were retained for further analysis using Ingenuity Pathway Analysis (IPA) software (Ingenuity Systems) as detailed in the online supplemental materials and methods.

RESULTS

Combination of acasunlimab and pembrolizumab potentiates T-cell proliferation, cytokine secretion and cytotoxic activity in vitro

To investigate whether additional PD-1 blockade can enhance the single-agent effects of acasunlimab on T-cell activation and cytotoxicity, the combination of acasunlimab with pembrolizumab was studied in vitro using MLR and antigen-specific T-cell assays (online supplemental figure 1).

Co-cultures of mDCs with purified allogeneic CD8⁺ T cells were treated with test and control antibodies across a range of concentrations (online supplemental figure 1A). Acasunlimab exerted single-agent activity indicative of immune activation in all three allogeneic donor pairs, showing a significant concentration-dependent increase in IL-2 and interferon gamma (IFN γ) release (figure 1A, online supplemental figure 4; online supplemental data file 1). The effects of pembrolizumab were significant for IFN γ and negligible for IL-2 secretion. Acasunlimab in combination with pembrolizumab strongly potentiated IL-2 and, to

a lesser extent, IFN γ secretion relative to each antibody alone, which was predicted to be synergistic in all tested donor pairs as defined by the HSA synergy model (HSA synergy scores > 10 ; figure 1B).

Since 4-1BB and PD-1 are coexpressed on exhausted antigen-experienced T cells,^{5 12–15} we evaluated the ability of concurrent 4-1BB agonism and PD-1/PD-L1 blockade to reinvigorate T_{dys}. An in vitro model for T_{dys} was generated by repeated CD3/CD28 stimulation of CD3⁺ T cells (online supplemental figure 1A) resulting in a T-cell phenotype resembling that of exhausted T cells (online supplemental figure 2A–C). These cells exhibited strongly reduced IFN γ secretion compared with functional T cells when co-cultured with mDCs (online supplemental figure 2D; $> 90\%$ average decrease). In the MLR assay with T_{dys}, acasunlimab increased secretion of IFN γ in all donors tested (figure 1C) and IL-2 in three out of four donors (online supplemental figure 2E,F; online supplemental data file 1). Pembrolizumab also induced secretion of IFN γ by T_{dys} but had a limited effect on IL-2 secretion. The combination of acasunlimab with pembrolizumab potentiated IFN γ secretion compared with either single agent, and was predicted to be synergistic in three out of four donor pairs at clinically relevant acasunlimab concentrations (0.1 to 10 $\mu\text{g/mL}$)^{25 28} (figure 1D). The combination also enhanced IL-2 secretion, with a predicted synergistic effect in two out of four donors (online supplemental figure 2G). Together, these results indicate that the combination of acasunlimab and an anti-PD-1 antibody can potentiate cytokine secretion by functional T cells and reinvigorate cytokine release by T_{dys} in vitro.

Next, we evaluated the effect of acasunlimab and pembrolizumab on T-cell proliferation and cytokine secretion in an antigen-specific setting, where human CD8⁺ T cells, engineered to express a CLDN6-specific TCR and high levels of PD-1, were co-cultured with autologous iDCs expressing the cognate antigen CLDN6 (online supplemental figure 1B). Acasunlimab significantly enhanced T-cell proliferation in a concentration-dependent manner (figure 2A; Online supplemental figure 5A; online supplemental data file 1). The effect of acasunlimab on T-cell proliferation was further enhanced when combined with pembrolizumab. The combination was predicted to be synergistic across the broad range of tested acasunlimab concentrations (figure 2B) with most prominent effects at low to intermediate concentrations ($\leq 0.4 \mu\text{g/mL}$) in all four donors (online supplemental figure 5B). Additionally, the acasunlimab-induced increase in IFN γ and IL-2 secretion (online supplemental data file 1) was further enhanced when combined with pembrolizumab (figure 2C) with synergistic effects predicted in all three donors tested (online supplemental figure 5C,D).

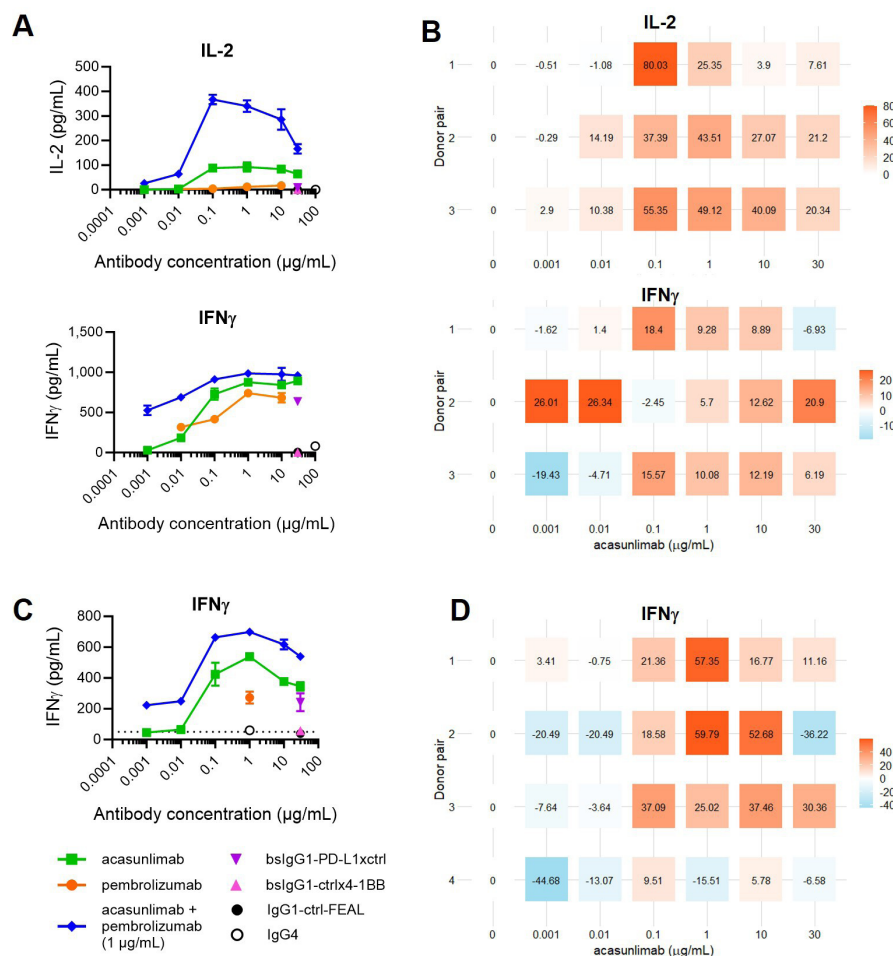


Figure 1 Potentiation of cytokine secretion by combining acasunlimab and pembrolizumab in MLR assays. MLR assay (online supplemental figure 1A) in co-cultures of mDC with purified CD8⁺ T cells (A, B) or co-cultures of mDC with dysfunctional CD3⁺ T cells (C, D) incubated with acasunlimab, pembrolizumab or the combination thereof (acasunlimab + 1 μg/mL pembrolizumab). (A) Mean IL-2 or IFN γ secretion in purified CD8⁺ T cell MLRs from one representative donor pair (donor pair 1) is shown with in (B) the corresponding HSA scores of all donor pairs tested (n=3). (C) Mean IFN γ secretion from one representative donor pair (donor pair 3) in MLRs with T_{dys} with in (D) the respective HSA synergy scores of all donor pairs tested (n=4). Scores >10 are considered predictive of synergy (B, D). Error bars denote SD of duplicate wells. HSA, Highest Single Agent; IFN γ , interferon gamma; IL-2, interleukin 2; mDC, mature dendritic cell; MLR, mixed lymphocyte reaction; PD-L1, programmed death-ligand 1; T_{dys}, dysfunctional T cells.

In an *in vitro* antigen-specific cytotoxicity assay, CLDN6-TCR⁺/PD-1⁺ CD8⁺ T cells were co-cultured with PD-L1⁺ MDA-MB-231 tumor cells expressing CLDN6 (online supplemental figure 1C). Acasunlimab significantly increased CD8⁺ T-cell mediated tumor-cell killing ($p < 0.05$ for 0.0033 μg/mL, that is, EC₂₀ concentration acasunlimab, vs control; **figure 2D**, online supplemental figure 6A). This effect was further enhanced when acasunlimab was combined with pembrolizumab, which had no significant effect as a single agent ($p < 0.05$ combination vs 0.015 μg/mL acasunlimab; $p < 0.01$ combination vs pembrolizumab). Additionally, the combination further potentiated the proportion of CD107a⁺GZMB⁺ CD8⁺ T cells relative to each single agent (online supplemental figure 6B).

Together, these results show that combining acasunlimab with an anti-PD-1 antibody potentiates the

proliferation, cytokine secretion and cytotoxic activity of antigen-specific CD8⁺ T cells.

Combination of anti-mPD-L1×m4-1BB and anti-mPD-1 potentiates antitumor activity *in vivo* across multiple syngeneic mouse tumor models with distinct tumor biology

As acasunlimab and pembrolizumab are not mouse-cross-reactive, *in vivo* antitumor activity of the combination was evaluated using an Fc-inert mouse IgG2a surrogate bispecific antibody targeting mouse PD-L1 and mouse 4-1BB (anti-mPD-L1×m4-1BB)²⁴ and anti-mPD-1 antibody clone RMP1-14 in syngeneic mouse models.

An mBPK/RO was developed to predict the amount of trimers formed by anti-mPD-L1×m4-1BB when simultaneously bound to 4-1BB and PD-L1 relative to the number of disrupted PD-1/PD-L1 complexes at different doses of anti-mPD-L1×m4-1BB in presence or absence of anti-mPD-1 (**figure 3A**). Optimal trimer

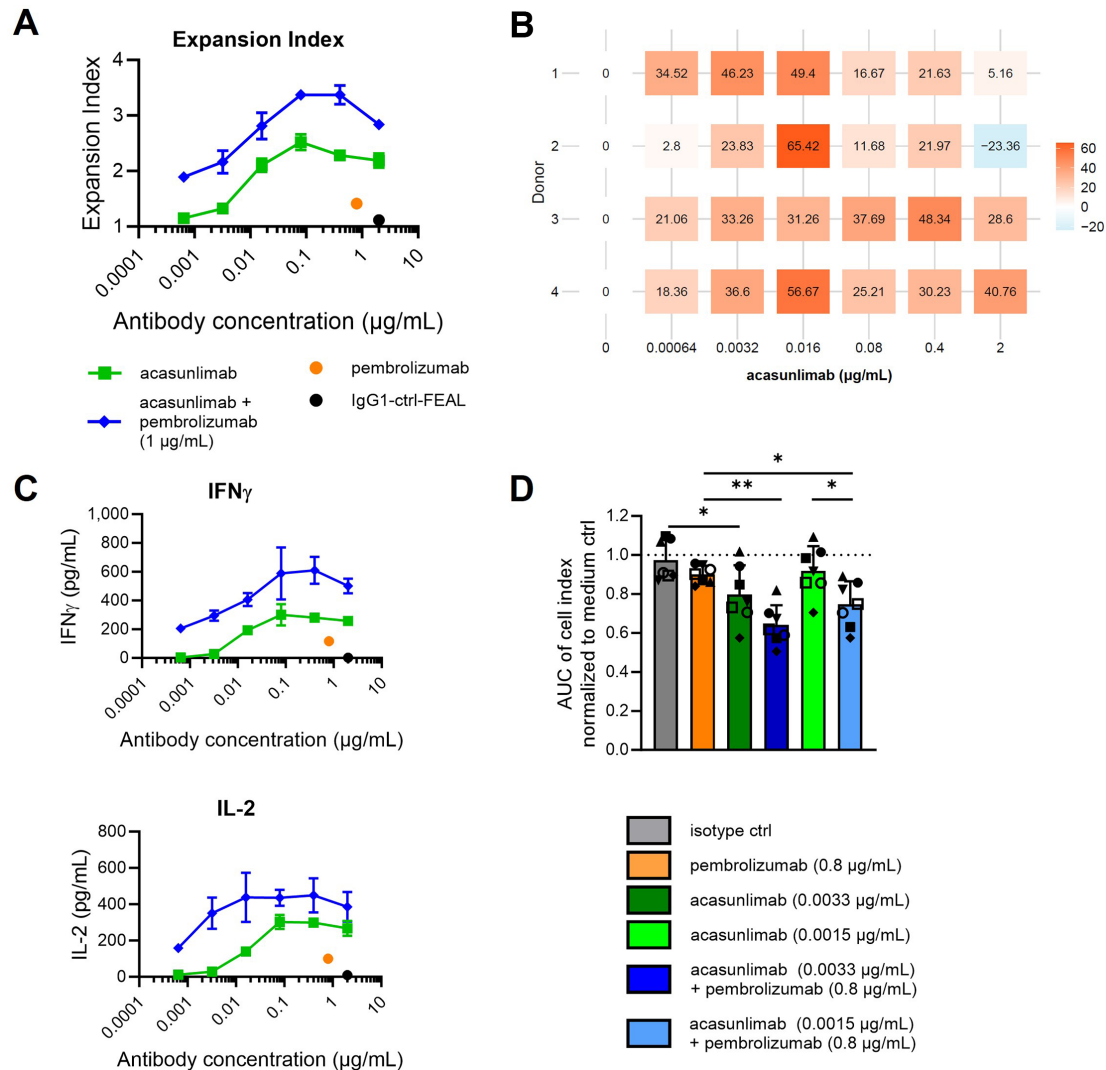


Figure 2 Potentiation of antigen-specific T-cell proliferation, cytokine secretion and cytotoxicity by combining acasunlimab and pembrolizumab in vitro. (A–C) CFSE-labeled human CLDN6-TCR⁺ PD-1⁺ CD8⁺ T cells incubated with CLDN6⁺ iDCs in the presence of acasunlimab in combination with pembrolizumab (0.8 μg/mL) (online supplemental figure 1B). (A) T-cell proliferation as determined by flow cytometry analysis of CFSE label dilution, expressed as mean expansion index \pm SD of duplicate wells of one representative donor (donor 3). (B) HSA synergy scores for the expansion index of all donors (n=4) with scores>10 considered as predictive of synergy. (C) Mean IFN γ and IL-2 secretion \pm SD of duplicate wells of one representative donor. (D) CLDN6-TCR⁺PD-1⁺ CD8⁺ T cells were co-cultured with previously seeded MDA-MB-231_hCLDN6 tumor cells (hCLDN6⁺ PD-L1⁺) in the presence of 0.0033 or 0.0015 μg/mL acasunlimab, 0.8 μg/mL pembrolizumab or the combination thereof (online supplemental figure 1C). Cytotoxicity of the CD8⁺ T cells toward MDA-MB-231_CLDN6 cells was monitored by electrical impedance measurement over 140–170 hours using the xCELLigence real-time cell analysis. Data were normalized to the time point of co-culture start and expressed relative to co-cultures incubated without antibodies, which was set to 100%. AUC (total area) analysis of normalized data is shown as mean \pm SD (n=6–7). Friedman test with Dunn's multiple comparison test was used to compare AUC between treatment groups (*p<0.05, **p<0.01). AUC, area under the curve; CFSE, carboxyfluorescein succinimidyl ester; hCLDN6, human Claudin-6; iDCs, immature dendritic cells; IFN γ , interferon gamma; IL-2, interleukin 2; PD-1, programmed cell death protein-1; TCR, T-cell receptor.

formation, and consequently optimal 4-1BB activation, was predicted to occur in the dose range of 1–5 mg/kg anti-mPD-L1 \times m4-1BB. However, the disruption of PD-1/PD-L1 complexes was incomplete (27–87%) at these doses (online supplemental table 1), similar to the bell-shaped response previously described for acasunlimab.²⁸ Increasing the dose of anti-mPD-L1 \times m4-1BB further enhanced the disruption of PD-1/PD-L1 complexes at the expense of trimer formation, resulting in reduced

4-1BB stimulation. In contrast, adding 10 mg/kg of anti-mPD-1 was predicted to disrupt more than 99% of the PD-1/PD-L1 complexes per T cell without impacting trimer formation at any anti-mPD-L1 \times m4-1BB dose level (figure 3A; online supplemental table 2). According to the model, 5 mg/kg anti-mPD-L1 \times m4-1BB falls within the peak range of trimer formation while also achieving substantial disruption of PD-1/PD-L1 complexes (87%; online supplemental table 1). Therefore, this dose

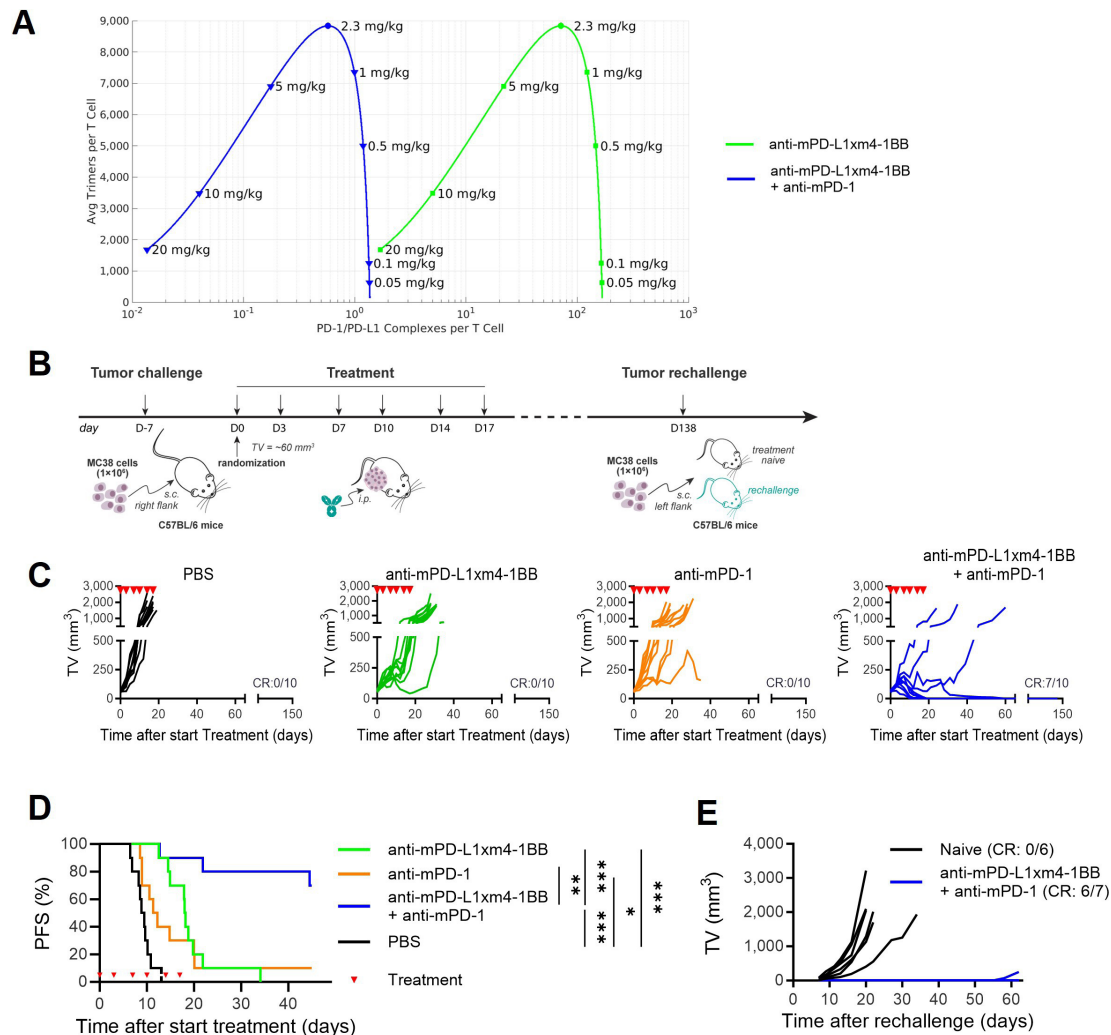


Figure 3 Therapeutic efficacy and memory response of anti-mPD-L1xm4-1BB and anti-mPD-1 combination in MC38 tumor-bearing mice. (A) mPBPK/RO model predictions of 4-1BB and PD-L1 engagement. Simulations were performed for anti-mPD-L1xm4-1BB monotherapy (0.05–20 mg/kg) and combination with anti-mPD-1 (10 mg/kg). Shown is the amount of 4-1BB/anti-mPD-L1xm4-1BB/PD-L1-crosslinked trimers formed versus the number of PD-1/PD-L1 complexes disrupted. (B) 1×10^6 MC38 tumor cells were injected SC in the right flank of C57BL/6 mice. After tumor establishment (60 mm³ average tumor volume), mice were randomized and treated with PBS, anti-mPD-L1xm4-1BB (5 mg/kg), anti-mPD-1 (10 mg/kg) or the combination thereof at the indicated time points (n=10 per group). (C) Tumor growth of individual mice in each group. CR: number of animals with a complete response. (D) PFS, defined as the percentage of mice with tumor volume smaller than 500 mm³, is shown as a Kaplan–Meier curve. Mantel–Cox analysis was used to compare PFS between treatment groups (*p<0.05, **p<0.01, ***p<0.001). (E) Mice with a CR after combination treatment (shown in C) were rechallenged by SC injection of 1×10^6 MC38 cells in the left flank 138 days after start treatment. As a control group, a second cohort of naïve mice was inoculated with 1×10^6 tumor cells. Tumor growth of individual mice in each group is shown. Results are representative of three independent experiments. i.p., intraperitoneal; mPBPK/RO, minimal physiologically-based pharmacokinetic model with receptor occupancy; PBS, phosphate-buffered saline; PD-1, programmed cell death protein-1; PD-L1, programmed death-ligand 1; PFS, progression-free survival; SC, subcutaneous; TV, tumor volume.

was selected as the preferred dose in follow-up in vivo studies.

In MC38 tumor-bearing C57BL/6 mice, single-agent treatment with 5 mg/kg anti-mPD-L1xm4-1BB or 10 mg/kg anti-mPD-1 delayed tumor outgrowth (figure 3B,C), as evidenced by a lower tumor growth rate (p<0.0001 vs control; online supplemental figure 7) and increased PFS relative to the control group (p<0.001 and p=0.012, respectively; figure 3D). The antitumor activity was potentiated when anti-mPD-L1xm4-1BB was combined

with anti-mPD-1 resulting in a lower tumor growth rate (p<0.005; online supplemental figure 7) and enhanced PFS (p<0.01; figure 3D) relative to each single agent. Notably, durable CR (no palpable tumor left) was observed in 7/10 mice treated with the combination, but in none of the mice treated with the single agent (figure 3C), indicating therapeutic synergy. After rechallenging these seven tumor-free mice with MC38 tumor cells on day 138 after the initial start of treatment, tumor outgrowth was suppressed with no tumors observed in

6/7 mice during the entire follow-up period of 63 days (figure 3E). Together, these data are consistent with a protective immune memory response in mice treated with the combination of anti-mPD-L1×m4-1BB and anti-mPD-1.

Antitumor activity of anti-mPD-L1×m4-1BB in combination with anti-mPD-1 was confirmed in three additional syngeneic models selected to represent TME diversity. In the MB49 urothelial carcinoma model that is characterized by high immune infiltration and known to be responsive to CPIs,³⁴ tumor growth was delayed and PFS increased by anti-mPD-L1×m4-1BB and anti-mPD-1 as single agents ($p<0.0001$ vs control; online supplemental figure 8). The antitumor activity was further enhanced when anti-mPD-L1×m4-1BB was combined with anti-mPD-1, resulting in a reduced tumor growth rate and extended PFS compared with each single agent ($p<0.05$ vs anti-mPD-L1×m4-1BB, $p<0.01$ vs anti-mPD-1). In the immunologically cold CPI-resistant B16F10 melanoma model,^{34,35} modest single-agent activity was only observed for anti-mPD-L1×m4-1BB, resulting in reduced tumor growth rate ($p<0.05$ vs control; online supplemental figure 9). Combining anti-mPD-L1×m4-1BB with anti-mPD-1 tended to further enhance tumor growth inhibition ($p<0.01$ vs control). While anti-mPD-L1×m4-1BB showed a trend of increased PFS ($p=0.06$ vs control), PFS was significantly extended by the combination ($p<0.001$ vs control). Finally, in the highly immunosuppressive Pan02 pancreatic ductal adenocarcinoma model that is resistant to anti-PD-(L)1 therapy,^{35,36} only the combination of anti-mPD-L1×m4-1BB and anti-mPD-1 reduced tumor growth rate ($p<0.05$ vs control) whereas the single-agent treatments did not (online supplemental figure 10). PFS was increased by anti-mPD-L1×m4-1BB single agent ($p<0.05$ vs control), which tended to be further extended when anti-mPD-L1×m4-1BB was combined with anti-mPD-1 ($p<0.001$ vs control). These findings from diverse syngeneic tumor models support potentiation of antitumor activity by the combination of anti-mPD-L1×m4-1BB and anti-mPD-1, with more pronounced effects in tumor models with pre-existing immune infiltration.

Combination of chi-acasunlimab and pembrolizumab potentiates antitumor activity in vivo in a mouse model expressing the human targets h4-1BB, hPD-L1 and hPD-1

To evaluate the in vivo effect of the combination in a model closer to the human setting, hPD-1/hPD-L1/h4-1BB tKI mice expressing the human targets were treated with chi-acasunlimab and pembrolizumab. Chi-acasunlimab was shown to block PD-1/PD-L1 and induce 4-1BB agonist activity in cell-based reporter assays and to activate T cells in human PBMC cultures in vitro to the same level as acasunlimab (online supplemental figure 11). Treating MC38-hPD-L1 tumor-bearing tKI mice with 5 mg/kg chi-acasunlimab and/or 10 mg/kg pembrolizumab was well tolerated, as no body weight loss (online supplemental figure 12A) nor clinical observations were reported. Tumor outgrowth was delayed relative to isotype

control in mice treated with chi-acasunlimab or pembrolizumab, with CR in 5/8 and 2/8 mice, respectively, which was also reflected by increased PFS ($p<0.001$ vs control) and decreased tumor growth rate (figure 4A–C, online supplemental figure 12B). When chi-acasunlimab was combined with pembrolizumab, tumor outgrowth inhibition resulting in CR was increased to 7/8 mice and PFS was further extended ($p=0.006$ vs pembrolizumab, $p=0.218$ vs chi-acasunlimab). All animals with a CR (pembrolizumab: $n=2$; chi-acasunlimab: $n=5$; combination: $n=7$) were protected from tumor outgrowth on rechallenge with MC38-hPD-L1 tumor cells on day 143 after the initial start of treatment (figure 4D), consistent with a protective immune memory response. Notably, the percentage of intratumoral cells expressing PD-L2 increased on day 5 after starting chi-acasunlimab-containing treatment (either alone or in combination with pembrolizumab) compared with the control and pembrolizumab-only groups (online supplemental figure 12C). Together, these data further support the rationale for combining acasunlimab with an anti-PD-1 agent to achieve full PD-1 blockade and inhibit the compensatory PD-1/PD-L2 pathway.

Next, the role of human PD-L1 expression on tumor cells in the antitumor activity of the combination of chi-acasunlimab with pembrolizumab was assessed using the hPD-1/hPD-L1/h4-1BB tKI mice implanted with MC38 WT tumor cells. Although antitumor activity was reduced compared with the MC38-hPD-L1-bearing tKI model, delayed outgrowth of MC38 WT tumors was observed in tKI mice treated with either 10 mg/kg chi-acasunlimab or 10 mg/kg pembrolizumab, resulting in increased PFS ($p<0.05$ vs control), 1 CR in each group, and decreased tumor growth rate for chi-acasunlimab ($p<0.05$ vs control) (online supplemental figure 13). The combination of chi-acasunlimab with pembrolizumab tended to further delay tumor outgrowth, evidenced by a more significant increase in PFS and decrease in tumor growth rate compared with the isotype control ($p<0.001$), and reduced tumor growth rate compared with chi-acasunlimab alone ($p<0.01$). However, PFS in the combination group was not significantly improved compared with the single-agent treatments. Since chi-acasunlimab and pembrolizumab bind only to host cells expressing the human targets in the tKI mice, but not the transplanted MC38 WT tumor cells that express endogenous mouse PD-L1 but lack human targets, these data suggest that the stronger antitumor activity observed in the MC38-hPD-L1 tumor-bearing tKI mice was, at least partially, dependent on the expression of hPD-L1 on the tumor cells.

Anti-mPD-L1×m4-1BB and anti-mPD-1 combination induces tumor antigen-specific T-cell expansion in vivo and increases intratumoral cytotoxic CD8⁺ TILs

Since most tumors in the MC38-hPD-L1 tumor-bearing tKI model were eradicated early on with combination treatment, the MC38-tumor-bearing C57BL/6 mouse model was used for in vivo MoA studies to allow a

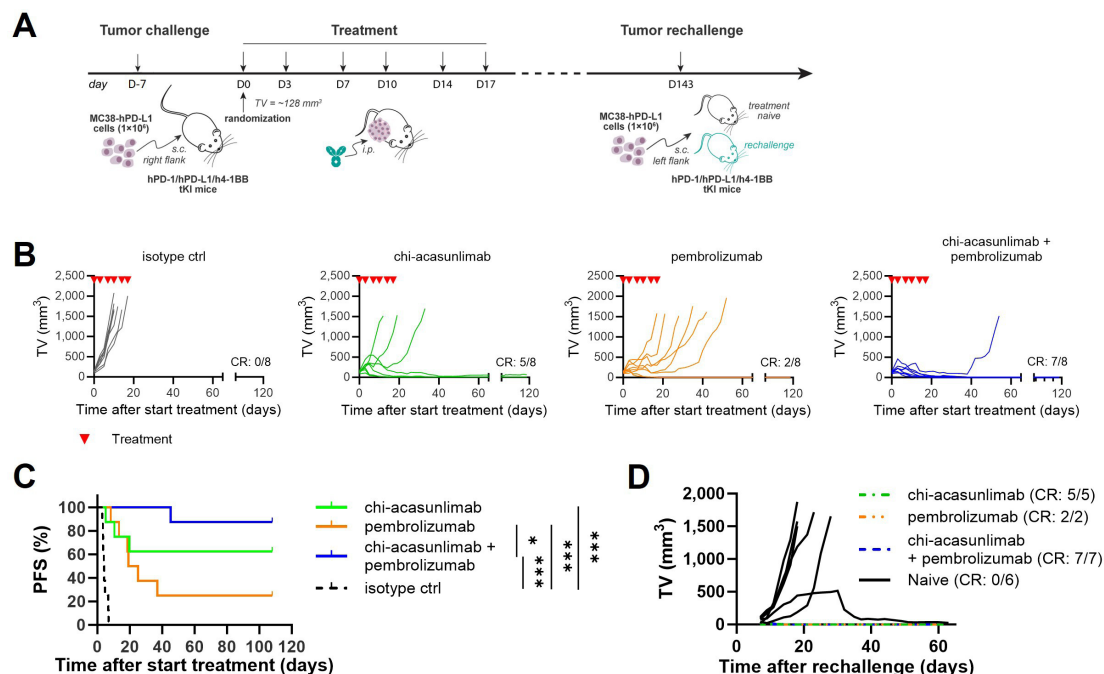


Figure 4 Therapeutic efficacy and memory response of chi-acasunlimab and pembrolizumab combination in MC38-hPD-L1 tumor-bearing hPD-1/hPD-L1/h4-1BB tKI mice. (A) 1×10^6 MC38-hPD-L1 tumor cells were injected SC in the right flank of hPD-1/hPD-L1/h4-1BB tKI mice. After tumor establishment (128 mm³ average tumor volume), mice were randomized and treated with isotype control antibodies (5 mg/kg mIgG2a + 10 mg/kg IgG4), chi-acasunlimab (5 mg/kg), pembrolizumab (10 mg/kg) or the combination thereof at the indicated time points ($n=8$ per group). (B) Tumor growth of individual mice in each group. CR: number of animals with a complete response. (C) PFS, defined as the percentage of mice with tumor volume smaller than 500 mm³, is shown as a Kaplan–Meier curve. Mantel–Cox analysis was used to compare PFS between treatment groups, with $*p<0.05$, $**p<0.01$, $***p<0.001$. (D) Mice with a CR after treatment (shown in B) were rechallenged by SC injection of 1×10^6 MC38-hPD-L1 cells in the left flank 143 days after start treatment. As a control group, a second cohort of naïve hPD-1/hPD-L1/h4-1BB tKI mice was inoculated with 1×10^6 tumor cells. Tumor growth of individual mice in each group is shown. PFS, progression-free survival; SC, subcutaneous; tKI, triple knock-in; TV, tumor volume.

sufficient window for studying the combination's effects. Tumor tissue, tdLNs and plasma were obtained from several studies on day 7 and/or day 14 after the start of treatment to perform various analyses, including IHC, flow cytometry, TCR and RNA sequencing, and cytokine measurements (online supplemental figure 14A,B).

IHC analysis of tumors collected on day 14 showed that each anti-mPD-L1 \times m4-1BB and anti-mPD-1 alone increased the percentage of CD3⁺ and CD8⁺ T cells ($p<0.05$ vs control), with the combination treatment further enhancing this effect ($p<0.05$ vs both single agents) (figure 5A). While anti-mPD-L1 \times m4-1BB did not affect the percentage of CD4⁺ T cells, this was increased by single-agent anti-mPD-1 ($p<0.01$ vs control) and combination treatment ($p<0.01$ vs control; $p<0.05$ vs anti-mPD-L1 \times m4-1BB). The observed increase in total CD4⁺ T cells was accompanied by increased percentages of FoxP3⁺ cells, indicative of T regulatory cells (Tregs) (online supplemental figure 14C). Across treatment groups, the increased percentages of intratumoral T cells inversely correlated with tumor volume (Spearman correlation, $r=-0.8$, $p<0.0001$; online supplemental table 3), suggesting a key role in tumor growth inhibition. The ratio of CD8⁺/FoxP3⁺ T cells was higher in the anti-mPD-L1 \times m4-1BB and combination treatment groups than

in the control and anti-mPD-1 groups ($p<0.01$; online supplemental figure 14C), indicating a favorable balance between effector and regulatory T cells.

Flow cytometry analysis of tdLNs collected on day 7 showed that anti-mPD-L1 \times m4-1BB increased CD3⁺, CD4⁺ and CD8⁺ T-cell numbers ($p<0.05$ vs control), which tended to be further enhanced by the combination with anti-mPD-1 ($p<0.001$ vs control; figure 5B). TCRseq analyses on day 7 revealed that the combination significantly reduced TCR diversity in the tdLNs relative to the single-agent groups, while no significant changes were observed in the tumor (figure 5C; online supplemental data file 2). Additionally, the tdLNs of mice treated with the combination showed an increased abundance of the top TCR clonotypes (online supplemental figure 14D). Reduced TCR diversity, along with increased T-cell numbers, suggested that the combination preferentially expanded tumor antigen-specific T cells in the tdLNs. Indeed, flow cytometry analyses using dextramers recognizing the immunodominant tumor antigens Adpgk, Repl1 and Rpl18 showed increased numbers of dextramer⁺ CD8⁺ T cells in the tdLNs on the anti-mPD-L1 \times m4-1BB and anti-mPD-1 single-agent treatments ($p<0.01$ vs control), which tended to be further increased on combination treatment ($p<0.001$ vs control and $p<0.05$ vs anti-mPD-1) and was

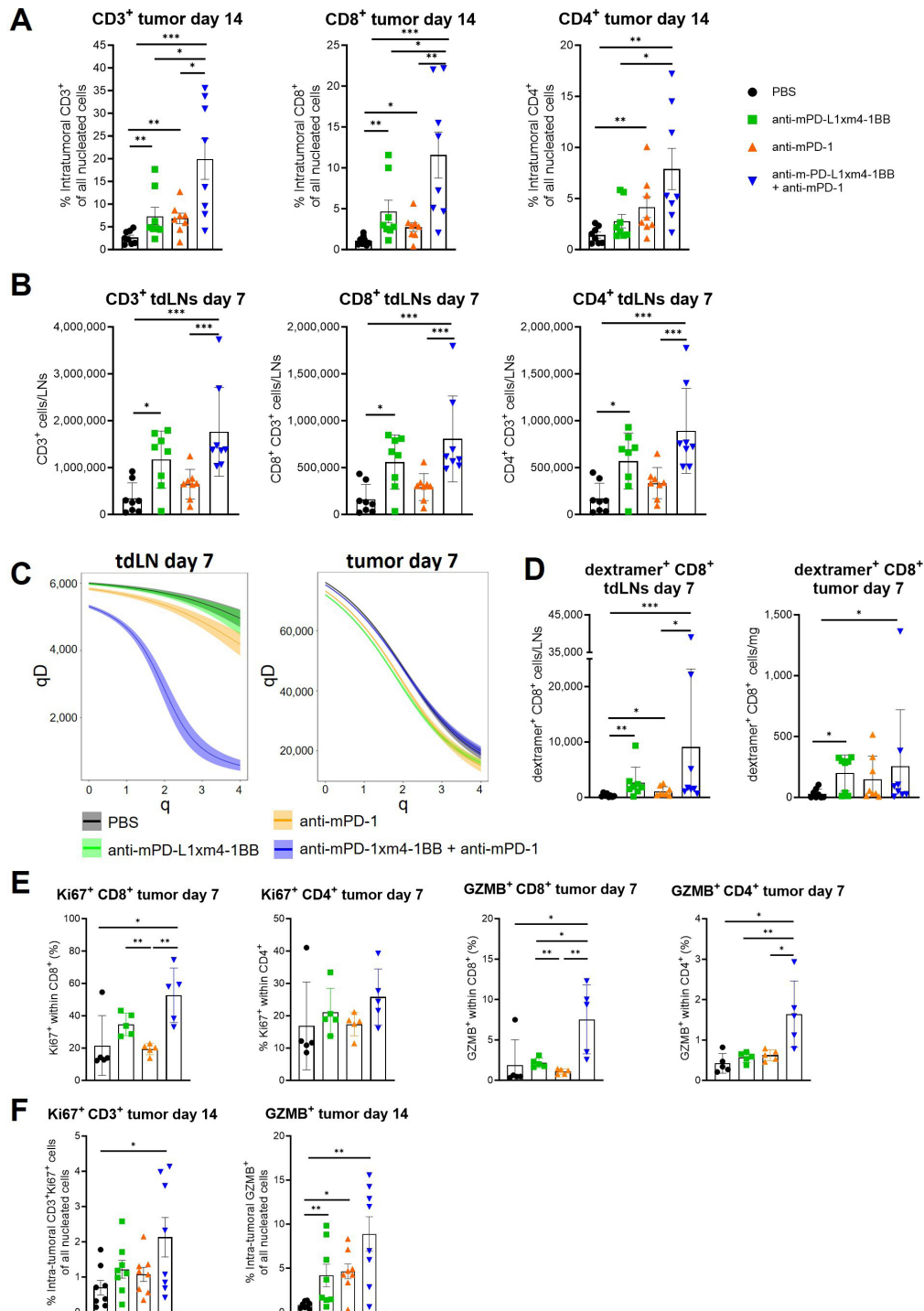


Figure 5 T-cell clonal expansion and enhanced cytotoxic CD8⁺ T-cell density induced by anti-mPD-L1xm4-1BB and anti-mPD-1 combination in MC38 tumor-bearing mice. Mice bearing MC38 tumors (50–70 mm³ average tumor volume) were treated with PBS, anti-mPD-L1xm4-1BB (5 mg/kg), anti-mPD-1 (10 mg/kg) or the combination thereof (2QWx2). (A) Sections of tumors (day 14) were analyzed by IHC to assess the percentage of CD3⁺, CD4⁺ and CD8⁺ cells among all nucleated cells. (B) Numbers of CD3⁺, CD4⁺ and CD8⁺ T cells in tumor-draining lymph nodes (tdLNs) (day 7) were analyzed by flow cytometry. (C) DNA extracted from tdLNs and tumor samples (day 7) were analyzed by TCR sequencing. Data shown are Hill diversity profiles of tdLN and tumor TCR repertoires. The diversity profile of each group is represented and displays the diversity values (qD) relative to each diversity order (q). Statistical comparison is provided in online supplemental data file 2. (D) Numbers of Adpgk, Repl1, and Rpl18 tumor antigen-specific (dextramer⁺) CD8⁺ T cells in tdLNs and tumor (day 7) were analyzed by flow cytometry. (E) Percentage Ki67⁺ and GZMB⁺ cells in total CD8⁺ and CD4⁺ populations in the tumors (day 7) were measured by flow cytometry. (F) Sections of tumors (day 14) were analyzed by IHC to assess the percentages of CD3⁺Ki67⁺ and GZMB⁺ cells among all nucleated cells. Mann-Whitney U statistical analysis was performed to compare between treatment groups (*p<0.05, **p<0.01, ***p<0.001). IHC, immunohistochemistry; LNs, lymph nodes; PBS, phosphate-buffered saline; 2QWx2, twice weekly for 2 weeks; TCR, T-cell receptor.

particularly pronounced in two mice in the combination group (figure 5D). Within the tumors, broadly comparable increased numbers of dextramer⁺ CD8⁺ T cells were observed in the anti-mPD-L1×m4-1BB single-agent and combination treatment groups ($p<0.05$ vs control). These data suggest that at early time points, the combination of anti-mPD-L1×m4-1BB with anti-mPD-1 promoted clonal expansion of tumor-antigen specific T cells primarily in the tDLNs.

Further evaluation of the functional properties of intratumoral CD8⁺ and CD4⁺ T cells by flow cytometry showed an increased proportion of proliferative (Ki67⁺) CD8⁺ TILs in the tumors in response to the combination of anti-mPD-L1×m4-1BB and anti-mPD-1 on day 7 ($p<0.05$ vs control and vs anti-mPD-1), whereas this population was not significantly modulated by either single-agent treatment (figure 5E). Consistently, an increased proportion of intratumoral Ki67⁺ CD3⁺ T cells was observed only for the combination treatment group in IHC analyses on day 14 ($p<0.05$ vs control; figure 5F). The proportion of cytotoxic (GZMB⁺) CD8⁺ and CD4⁺ T cells was also increased by the combination treatment on day 7 relative to each single agent in the flow cytometry analysis ($p<0.05$; figure 5E). Furthermore, IHC analyses suggested that increased proportions of bulk intratumoral GZMB⁺ cells may be maintained on day 14 ($p<0.05$ single agents vs control; $p<0.01$ combination vs control; median combination fold-increase >2 vs both single agents; figure 5F). Across all treatment groups, the proportion of Ki67⁺ CD8⁺ and GZMB⁺ CD8⁺ T cells in the tumor on day 7 (determined by flow cytometry), and GZMB⁺ cells in the tumor on day 14 (determined by IHC) showed an inverse correlation with tumor volume ($p<0.05$; online supplemental table 3). These results suggest that the combination's antitumor activity was associated with enhanced T-cell proliferation and cytotoxicity in the tumor.

Anti-mPD-L1×m4-1BB and anti-mPD-1 combination potentiates IFN γ and IL-2 signaling in vivo and induces cytotoxic stem-like CD8⁺ T cell phenotype

To further investigate the underlying mechanisms of enhanced antitumor activity by the combination, bulk RNA sequencing and IPA analysis of tumor tissues collected from MC38-tumor bearing C57BL/6 mice after treatment for 7 days with anti-mPD-L1×m4-1BB and/or anti-mPD-1 were performed. The top 20 significantly represented canonical pathways in the combination group versus control, which showed the highest average Δp value compared with the two single-agent treatment arms versus control, included antigen presentation, IFN signaling, macrophage and Th1 and Th2 cell activation pathways (figure 6A). Interestingly, the IL-10 signaling pathway was also presented but had a negative z-score, indicating that it was predicted to be inhibited by combination treatment. Additionally, the top 20 upstream regulators predicted to be more significantly activated in the combination group compared with the two single-agent treatment arms included type I and type II IFNs (IFNG,

IFNA2, IFNB1) and their signaling molecules (STAT1, IRF1, IRF7, IRF3), DC-secreted cytokines (IL-12 and IL-27), and cytokines promoting natural killer and CD8⁺ T-cell cytotoxic functions (IL-21 and IL-15) (figure 6B). The predicted potentiation of IFN γ signaling in the tumor was supported by increased IFN γ plasma levels observed on day 7 after the start of treatment with the combination compared with the control group ($p<0.01$; figure 6C). In line with the above findings, the top 20 upstream regulators predicted to be inhibited by the combination treatment more significantly than each monotherapy group included multiple enzymes (*TREX1*, *DNASE2*, *PNPT1*, *IRGM*, *CLPP*) that, when inhibited, may promote antitumor immunity by enhancing STING-mediated type I IFN responses.^{37–41} Interestingly, this list also included *STAT6* and *PIK3CG*, known to promote immune-suppressive tumor-associated macrophages,^{42 43} *PRDM1*, involved in CD8⁺ T-cell exhaustion,⁴⁴ and *RC3H1* and *IL10RA*, encoding suppressors of CD8⁺ and CD4⁺ T-cell functions⁴⁵ (online supplemental figure 15). Altogether, these predictions suggest that the combination treatment enhances antitumor activity by mitigating inhibitory mechanisms (eg, IL-10 signaling and immune-suppressive macrophages) and enhancing T-cell priming and functions via both Th1-related and Th2-related signaling and reducing T-cell dysfunction.

Since IL-2 secretion was strongly increased by the combination of acasunlimab with pembrolizumab in the in vitro studies, the effects on the IL-2 signaling pathway in the MC38-tumor bearing C57BL/6 mouse model were further investigated using the tumor transcriptomic data. Combination treatment increased messenger RNA (mRNA) levels of *IL2RA* (CD25) ($p<0.05$), *IL2RB* (CD122) ($p<0.01$) and *IL2RG* (CD132) ($p<0.05$) compared with the control group (figure 6D; online supplemental figure 16A). Notably, *IL2RA* mRNA levels were not modulated by single-agent treatment with anti-mPD-L1×m4-1BB or anti-mPD-1. Additionally, the IL-2 signaling pathway was predicted by IPA to be enriched specifically in the tumors treated with the combination ($p<0.05$ vs control; online supplemental figure 16B,C), with *IL2RA* being one of the predicted key signaling nodes in the IPA interaction network analysis (online supplemental figure 16D). Involvement of IL-2 signaling in the effects of combination treatment was further supported by flow cytometry analysis of tumor samples collected on day 7, which showed increased CD25 expression levels on CD8⁺ T cells ($p<0.05$ vs all other groups) and increased proportions of intratumoral CD25⁺ CD8⁺ T cells ($p<0.05$ vs control and vs anti-mPD-1) (figure 6E). Moreover, the proportion of CD25⁺ CD8⁺ T cells in the tumor inversely correlated with tumor volume across all treatment groups ($p<0.01$; online supplemental table 3). In contrast, these tumor samples did not show significant changes in CD25 expression on CD4⁺ T cells (online supplemental figure 17A), nor in the proportion of Tregs (FoxP3⁺ CD4⁺ T cells) or CD25⁺ cells within the Treg subset (online supplemental figure 17B,C).

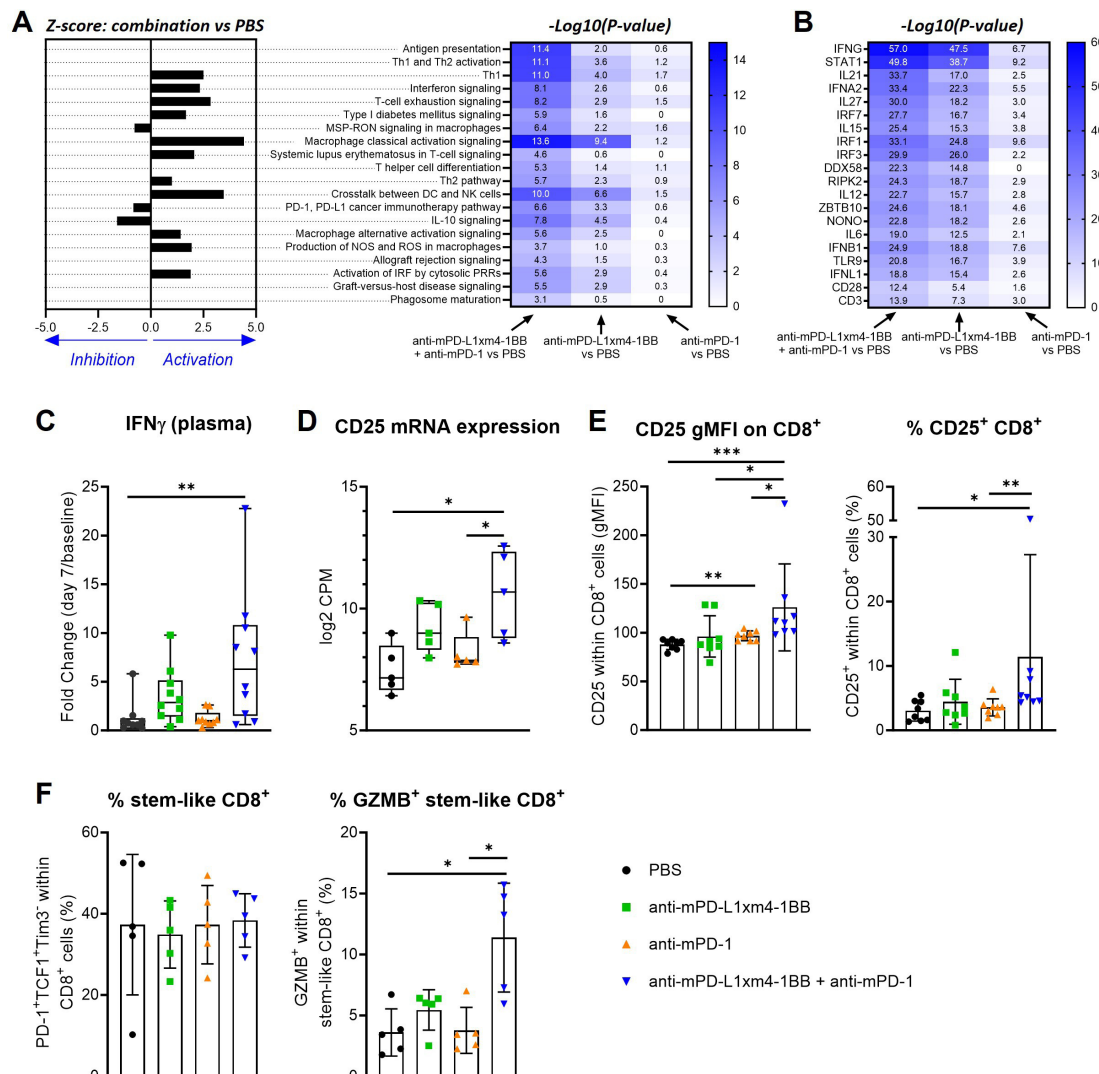


Figure 6 Modulation of key immune signaling pathways and induction of intratumoral cytotoxic stem-like CD8⁺ T cells by anti-mPD-L1xm4-1BB and anti-mPD-1 combination in MC38 tumor-bearing mice. (A, B) Differential gene expression with IPA pathway analysis on RNA extracted from tumors (day 7) was assessed for each treatment relative to the PBS control arm. (A) P value heatmap depicts the top 20 canonical pathways most significantly represented in the combination treatment compared with the single agents, including both activated and downregulated pathways. The bar chart indicates whether the pathways were predicted to be activated (positive z-score; right direction in bar diagram) or inhibited (negative z-score; left direction in bar diagram) by the combination treatment. If the direction of the effect could not be predicted, no z-score is displayed. (B) P value heatmap depicts the top 20 upstream regulators predicted to be more significantly activated by the combination treatment compared with the single agents. See online supplemental figure 15 for the top 20 inhibited upstream regulators. (C) Fold change IFN γ levels on day 7 over baseline in plasma. Treatment groups in (C) were compared by Kruskal-Wallis analysis (**p<0.01). (D, E) CD25 expression in tumors (day 7) was analyzed at (D) the mRNA (RNAseq) and (E) protein level on CD8⁺ T cells (flow cytometry). (F) CD8⁺ T cells in tumors (day 7) were further characterized by defining the percentage stem-like (PD-1⁺TCF1⁺Tim3⁺) and GZMB⁺ stem-like CD8⁺ T cells. Treatment groups in (D–F) were compared by Mann-Whitney U statistical analysis (*p<0.05, **p<0.01, ***p<0.001). CPM, counts per million; DC, dendritic cell; gMFI, geometric mean fluorescence intensity; IFN γ , interferon gamma; IPA, ingenuity pathway analysis; mRNA, messenger RNA; NK, natural killer; PBS, phosphate-buffered saline; PD-1, programmed cell death protein-1; PD-L1, programmed death-ligand 1.

IL-2/CD25 signaling has been recently described to play a pivotal role in mediating differentiation of stem-like CD8⁺ T cells into GZMB⁺ “better-effector” CD8⁺ T cells that are not fate-locked into the T-cell exhaustion program.^{4 15 46 47} Therefore, it was hypothesized that increased IL-2 signaling by the combination of anti-mPD-L1xm4-1BB and anti-mPD-1 may enhance the cytotoxic capacity of stem-like CD8⁺ T cells to potentiate antitumor

immunity. Flow cytometry analysis of tumors collected on day 7 showed that the percentage of intratumoral stem-like (PD-1⁺TCF1⁺TIM3⁺) CD8⁺ T cells was not affected by either single-agent or combination treatment. However, the percentage of GZMB⁺ stem-like CD8⁺ T cells, indicative of enhanced cytotoxic activity, was increased by the combination relative to control (p<0.05), anti-mPD-L1xm4-1BB (p=0.056), and anti-mPD-1 (p<0.05)

(figure 6F). The proportion of GZMB⁺ stem-like CD8⁺ T cells correlated inversely with tumor volume across all treatment groups ($p < 0.001$; online supplemental table 3). The percentage of total or of GZMB⁺ intratumoral terminally differentiated (PD-1⁺TCF-1⁺TIM3⁺) CD8⁺ T cells was not significantly affected by single-agent nor combination treatment compared with control (online supplemental figure 17D,E). These results suggest that the anti-mPD-L1×m4-1BB and anti-mPD-1 combination could foster differentiation of stem-like CD8⁺ T cells into T cells with superior functional capacity (“better-effector T cells”) within the TME, which is associated with tumor outgrowth inhibition.

DISCUSSION

In this study, we found that combining acasunlimab with additional PD-1 blockade elicits complementary immune modulatory effects in both the tumor and tdLNs, leading to potent antitumor activity and protective immune responses. We hypothesize that several mechanisms contribute to the synergistic effects mediated by the combination. First, the combination can achieve optimum 4-1BB costimulation coupled with complete blockade of PD-1 signaling by inhibiting its interaction with both PD-L1 and PD-L2. As shown previously for acasunlimab,²⁸ dose levels of anti-mPD-L1×m4-1BB achieving maximal 4-1BB activation lead to partial PD-L1 blockade. Adding anti-mPD-1 fully disrupts PD-1/PD-L1 complexes, as predicted by mPBPK/RO modeling. Furthermore, chi-acasunlimab induced PD-L2 expression in the TME, underscoring the combination’s advantage of also blocking the compensatory PD-1/PD-L2 pathway. Second, while acasunlimab-driven 4-1BB activation requires crosslinking with PD-L1-expressing tumor or antigen-presenting cells (APCs) targeting it to the preferred site of action, anti-PD-1 may complement this by broadly targeting T cells throughout the TME, lymph nodes, and circulation, regardless of their involvement in the immune synapse, thereby amplifying the adaptive immune response.

Here, we observed that acasunlimab combined with pembrolizumab synergistically potentiated CD8⁺ T-cell functions and reinvigorated T_{dys}, leading to enhanced T-cell proliferation, activation (IFN γ and IL-2 secretion) and cytotoxic activity in vitro. In both WT and hPD-1/hPD-L1/h4-1BB tKI syngeneic mouse models, combination treatment potentiated antitumor activity, evidenced by prolonged survival, reduced tumor burden, a higher incidence of CRs, and tumor outgrowth protection on rechallenge, which is indicative of immune memory response. In the MC38 syngeneic mouse tumor model, the combination of anti-mPD-L1×m4-1BB and anti-mPD-1 antibodies significantly reduced TCR diversity and promoted clonal expansion of tumor-antigen specific T cells in the tdLNs. Within the TME, the combination enhanced CD8⁺ T-cell proliferation, potentiated IL-2 signaling, and increased the proportion of cytotoxic

stem-like CD8⁺ TILs thought to possess superior effector function.

Chronic antigen stimulation, such as during viral infections or tumor pathogenesis affects CD8⁺ T-cell proliferation and differentiation, resulting in subsets of CD8⁺ T cells at various functional states, including stem-like, transitory effector-like, and terminally differentiated (exhausted) CD8⁺ T cells.^{3,4} Specifically, antigen-driven proliferation and differentiation of quiescent stem-like PD-1⁺TCF-1⁺TIM3⁺ CD8⁺ T cells, also referred to as progenitor exhausted CD8⁺ T cells, result in transitory effector-like CD8⁺ T cells that exert effector functions on target cells, but will eventually give rise to terminally differentiated PD-1⁺TCF-1⁺TIM3⁺ CD8⁺ T cells, marking a trajectory towards CD8⁺ T cell exhaustion.^{5,48–51} While PD-1 inhibition triggers the proliferation of stem-like CD8⁺ T cells and their differentiation into transitory effector-like CD8⁺ T cells, exhausted T cells eventually accumulate.^{4–6} Here, we showed that combination treatment with anti-mPD-L1×m4-1BB and anti-mPD-1 preferentially potentiated the frequency of cytotoxic stem-like CD8⁺ T cells in the TME. These cytotoxic stem-like CD8⁺ T cells resemble “better effector” CD8⁺ T cells previously identified as highly functional effector CD8⁺ T cells that originate from a distinct differentiation program of stem-like CD8⁺ T cells that can be triggered by IL-2 signaling upon PD-1 blockade.^{4,15,46,47,52} The combination of acasunlimab with pembrolizumab strongly potentiated IL-2 secretion in CD8⁺ T-cell MLR and antigen-specific T-cell proliferation assays in vitro, while the combination of mouse-surrogate antibodies in vivo significantly increased the percentage of CD25⁺ CD8⁺ TILs, as well as CD25 expression levels on CD8⁺ T cells. This was corroborated by tumor transcriptomic analyses, which predicted enhanced IL-2 signaling in the TME in response to the combination therapy. Together, our data suggest that autocrine IL-2–CD25 signaling promotes the accumulation of tumor-specific cytotoxic stem-like CD8⁺ TILs, which may serve as key mediators of enhanced antitumor activity by the combination of acasunlimab with additional PD-1 blockade. This proposed MoA is consistent with coexpression of 4-1BB and PD-1 on stem-like CD8⁺ T cells,^{12,14,15,19} the ability of 4-1BB signaling to enhance IL-2 production and CD25 expression on T cells,^{53,54} and the pivotal role of CD25 engagement by IL-2 in the therapeutic synergy between PD-1 blockade and IL-2 cytokine treatment.^{4,47,55}

Our tumor transcriptomic analyses revealed enrichment of both Th1-related and Th2-related signaling gene signatures in response to the combination therapy. Emerging evidence suggests that, while Th1-mediated immunity has traditionally been considered the primary driver of antitumor responses, Th2 cells also play an important role through distinct mechanisms.⁵⁶ Importantly, Bai *et al* demonstrated that a deficit in Th2 functionality in anti-CD19 chimeric antigen receptor (CAR)-T cell infusion products was observed in patients with CD19⁺ acute lymphoblastic leukemia experiencing early relapse

on treatment.⁵⁷ This was associated with CAR-T over-differentiation into an effector phenotype, along with a diminished ability to sustain stem cell-like and central memory T-cell states, suggesting a role for Th2 signaling in maintaining T-cell functionality. Consistent with this, a recent preclinical study demonstrated that therapeutic strategies leveraging the type 2 cytokine IL-4 can reinvigorate exhausted CD8⁺ T cells in tumors and potentiate immune checkpoint blockade.⁵⁸ In this context, our data may indicate a broader modulation of the adaptive immune response induced by acasunlimab and anti-PD-1 combination, where Th2-cell-related cytokines and functions interplay with type 1 immunity in eliciting long-lasting antitumor responses.

Previous studies reported that 4-1BB agonism in Tregs may contribute to their expansion, though it does not appear to either enhance or inhibit their immunosuppressive functions.⁹ This could be explained by the fact that Tregs use IL-2 depletion as a dominant mechanism to suppress CD8⁺ T cells,⁵⁹ while 4-1BB signaling in conventional T cells drives IL-2 production to overcome this suppression.⁵³ Consistent with this, an increase in FoxP3⁺ cells was observed on combination therapy in our study, however, it correlated with enhanced infiltration of total CD4⁺ and CD8⁺ T cells and was accompanied by a favorable CD8⁺/FoxP3⁺ cell ratio. These data suggest that the enhanced Treg infiltration reflects a broad intratumoral inflammatory response induced by the combination. Future preclinical studies are needed to explore the potential role of tumoral FoxP3⁺ cells in the antitumor activity of the combination, for example, by adding an anti-CTLA-4 antibody that may inhibit or deplete Tregs in addition to enhancing T-cell priming. Prior preclinical work has demonstrated that the combination of 4-1BB agonism and CTLA-4 blockade potentiates antitumor immunity in animal models, including poorly immunogenic tumor models.^{60 61}

Our findings suggest that the tdLNs serve as an important site of action for the combination of anti-PD-L1×4-1BB and anti-PD-1 antibody therapies. PD-1 and 4-1BB are expressed on T cells and PD-L1 and PD-L2 are expressed on DCs in the tdLNs in patients and mouse models.^{62–64} In line with this, acasunlimab and other anti-PD-L1×4-1BB bispecific antibodies have been shown to strengthen the interaction between T cells and DCs.^{25 26} Stem-like CD8⁺ T cells in the tdLNs were identified as the primary targets of anti-PD-(L)1 therapy^{62 65 66} and their clonal expansion and trafficking to the tumor have been implicated in the clinical activity of PD-1 blockade in patients.^{50 51 64 67} Consistent with this, we observed that the combination of anti-mPD-L1×m4-1BB and anti-mPD-1 antibodies reduced TCR diversity and increased clonal expansion of tumor-antigen specific T cells in the tdLNs. In line with these in vivo mouse data, co-culture assays with human CD8⁺ T cells and DCs showed that the combination of acasunlimab and pembrolizumab synergistically potentiated T-cell expansion and cytokine release and was also able to reinvigorate T_{lys}. Together, these

data suggest that acasunlimab, in combination with an anti-PD-1 agent, promotes tumor-specific T-cell priming, clonal expansion, and reinvigoration of T_{lys}, by leveraging target coexpression in the tdLNs.

Collectively, our findings suggest distinct phases in the therapeutic effect elicited by acasunlimab combined with anti-PD-1, involving the tumor and the tdLNs. Antitumor activity might occur through amplifying pre-existing (tumor-specific) tumor-resident T cells, including reinvigoration of T_{lys}, as well as via stem-like CD8⁺ T cells trafficking from the tdLNs. Stem-like CD8⁺ T cells have indeed been reported to be primed in the tdLNs and infiltrate into the TME where they reside in dense APC niches and acquire the costimulation required to proliferate and differentiate into effector T cells for protective responses.^{50 68} Consistent with this, a recent study has described that conventional type 1 DCs deliver costimulation via the 4-1BB/4-1BBL axis, reinvigorating CD8⁺ T cells in the TME, which is required for the efficacy of PD-(L)1 blockade.⁶⁹ Our tumor transcriptomic analyses predicted enrichment of antigen presentation pathways and upstream regulators, such as IFN γ , type I IFNs and DC-secreted cytokines (ie, IL-12), in response to the combination therapy. This suggests that the combination may provide the required costimulation for stem-like CD8⁺ T cells to acquire effector functions within the TME, both directly through conditional 4-1BB agonist activity as well as indirectly by potentiating APC functions.

In conclusion, our results suggest that combining acasunlimab with additional PD-1 blockade may amplify the depth and the duration of antitumor immune responses. Consistent with the strong preclinical evidence presented here, the combination of acasunlimab and pembrolizumab demonstrated improved durability of clinical responses in an ongoing Phase 2 trial that enrolled patients with advanced metastatic non-small cell lung cancer (NSCLC) whose tumors express PD-L1 and who have progressed on prior CPI-containing therapy (NCT05117242).⁷⁰ Based on these encouraging results, a pivotal Phase 3 study evaluating the combination in PD-L1-positive metastatic NSCLC has been initiated (ABBIL1TY NSCLC-06; NCT06635824).

Acknowledgements The authors thank Eline Schipper-Steenwijk, Elke Gresnigt-van den Heuvel, Gaurav Bajaj, Gergő Fülöp, Gijs Zom, Jeroen van den Brakel, Joris van Sadelhoff, Marcel Brandhorst, Melissa Rutten, Nathan Cheadle and Omar Jabado of Genmab for their technical expertise. The authors thank Ann-Kathrin Wallisch and Natalie Schwarz of BioNTech for their technical expertise. Part of the material included in the manuscript has been presented at scientific conferences (AACR 2023, CIMT 2023 and SITC 2024): Capello M, Sette A, Plantinga T, et al. Abstract 3283: GEN1046 (DuoBody-PD-L1×4-1BB) in combination with PD-1 blockade potentiates anti-tumor immunity. Cancer Research 2023;83(7_Supplement):3283-83. doi: 10.1158/1538-7445.Am2023-3283 Capello M: GEN1046 (DuoBody-PD-L1×4-1BB) in combination with PD-1 blockade potentiates anti-tumor immunity. Oral presentation at the 20th CIMT Annual Meeting May 3-5, 2023; Mainz, Germany Capello M, Sette A, Plantinga TS, et al. 719 Acasunlimab combined with PD-1 blockade elicits complementary immune-modulatory effects and enhances anti-tumor activity in preclinical models. Journal for ImmunoTherapy of Cancer 2024;12(Suppl 2):A821-A21. doi: 10.1136/jitc-2024-SITC2024.0719

Contributors AM, AS, KBN, MJ-K, MC, MF, NP, ÖT, PGC, SF-K, TA and US contributed to conception of the work. AI, AS, JMB, KBN, MC, SF-K, TP and VMS

contributed to the study design and methodology. BWH, CCS, CJT, CY and VMS contributed to conduction of experiments, data acquisition, data curation or formal analysis of the data. AS, BWH, JMB, KBN, MC, NP and TP contributed to project administration and supervision. AI, AS, AT, BdAP, BWH, CJT, CY, JMB, KBN, KS, MC, SMB, TP and NP contributed to data visualization. AI, AS, AT, KBN, KS, MC, NP and SMB contributed to writing of the original draft, and all authors have revised the draft. NP is the guarantor.

Funding This study was funded by Genmab A/S and BioNTech SE.

Competing interests MC, AS, TP, CJT, VMS, JMB, BWH, PGC, CY, KS, SMB, TA, MF, MJ-K and NP are employees at Genmab and own stock and/or stock options. ÖT and US are management board members and employees at BioNTech SE. KBN, SF-K, AT, AI, BdAP, and AM are employees at BioNTech SE and have securities from BioNTech SE. AM, JMB, MJ-K, NP, PGC, SF-K and US are co-inventors on WO2023057534 (multispecific binding agents against PD-L1 and CD137 combination) and AM, MJ-K, NP and US are co-inventors on WO2023057535 (multispecific binding agents against PD-L1 and CD137 in combination with anti-PD-1 antibodies for treating cancers).

Patient consent for publication Not applicable.

Ethics approval All animal studies were performed at Crown Bioscience and approved by their Institutional Animal Care and Use Committee (IACUC). The protocol approval ID's are AN-2104-09-66, AN-2104-09-884, AN-2204-05-249, AN-2204-05-2152, AN-2304-07-0479, AN-2304-07-0798, AN-2401-03-0472, AN-2401-03-0471, and AN-2401-03-0570.

Provenance and peer review Not commissioned; externally peer reviewed.

Data availability statement Data are available upon reasonable request. Some materials and data sets generated and/or analyzed during the current study are not publicly available but could be made available under materials transfer agreements (MTAs) upon reasonable request to the corresponding author.

Supplemental material This content has been supplied by the author(s). It has not been vetted by BMJ Publishing Group Limited (BMJ) and may not have been peer-reviewed. Any opinions or recommendations discussed are solely those of the author(s) and are not endorsed by BMJ. BMJ disclaims all liability and responsibility arising from any reliance placed on the content. Where the content includes any translated material, BMJ does not warrant the accuracy and reliability of the translations (including but not limited to local regulations, clinical guidelines, terminology, drug names and drug dosages), and is not responsible for any error and/or omissions arising from translation and adaptation or otherwise.

Open access This is an open access article distributed in accordance with the Creative Commons Attribution Non Commercial (CC BY-NC 4.0) license, which permits others to distribute, remix, adapt, build upon this work non-commercially, and license their derivative works on different terms, provided the original work is properly cited, appropriate credit is given, any changes made indicated, and the use is non-commercial. See <http://creativecommons.org/licenses/by-nc/4.0/>.

ORCID iDs

Saskia M Burm <http://orcid.org/0000-0002-5000-2026>

Kristin Strumane <http://orcid.org/0009-0009-5910-9477>

Aras Tokar <http://orcid.org/0000-0001-6601-0939>

Andrea Imle <http://orcid.org/0000-0002-8740-1477>

REFERENCES

- Reck M, Rodríguez-Abreu D, Robinson AG, *et al.* Pembrolizumab versus Chemotherapy for PD-L1-Positive Non-Small-Cell Lung Cancer. *N Engl J Med* 2016;375:1823–33.
- Tawbi HA, Schadendorf D, Lipson EJ, *et al.* Relatlimab and Nivolumab versus Nivolumab in Untreated Advanced Melanoma. *N Engl J Med* 2022;386:24–34.
- Giles JR, Globig A-M, Kaech SM, *et al.* CD8+ T cells in the cancer-immunity cycle. *Immunity* 2023;56:2231–53.
- Hashimoto M, Ramalingam SS, Ahmed R. Harnessing CD8 T cell responses using PD-1-IL-2 combination therapy. *Trends Cancer* 2024;10:332–46.
- Miller BC, Sen DR, Al Abosy R, *et al.* Subsets of exhausted CD8+ T cells differentially mediate tumor control and respond to checkpoint blockade. *Nat Immunol* 2019;20:326–36.
- Pauken KE, Sammons MA, Odorizzi PM, *et al.* Epigenetic stability of exhausted T cells limits durability of reinvigoration by PD-1 blockade. *Science* 2016;354:1160–5.
- Choi Y, Shi Y, Haymaker CL, *et al.* T-cell agonists in cancer immunotherapy. *J Immunother Cancer* 2020;8:e000966.
- Horton BL, Williams JB, Cabanov A, *et al.* Intratumoral CD8+ T-cell Apoptosis Is a Major Component of T-cell Dysfunction and Impedes Antitumor Immunity. *Cancer Immunol Res* 2018;6:14–24.
- Melero I, Sanmamed MF, Glez-Vaz J, *et al.* CD137 (4-1BB)-Based Cancer Immunotherapy on Its 25th Anniversary. *Cancer Discov* 2023;13:552–69.
- Hosoi A, Takeda K, Nagaoka K, *et al.* Increased diversity with reduced “diversity evenness” of tumor infiltrating T-cells for the successful cancer immunotherapy. *Sci Rep* 2018;8:1058.
- Segal NH, Logan TF, Hodi FS, *et al.* Results from an Integrated Safety Analysis of Urelumab, an Agonist Anti-CD137 Monoclonal Antibody. *Clin Cancer Res* 2017;23:1929–36.
- Andreata M, Corria-Osorio J, Müller S, *et al.* Interpretation of T cell states from single-cell transcriptomics data using reference atlases. *Nat Commun* 2021;12:2965.
- Blum J, Spires V, Masters G, *et al.* DuoBody®-PD-L1x4-1BB (GEN1046) reverses T-cell exhaustion in vitro. *J Immunother Cancer* 2018;12:08.
- Pichler AC, Carrié N, Cuisinier M, *et al.* TCR-independent CD137 (4-1BB) signaling promotes CD8+ exhausted T cell proliferation and terminal differentiation. *Immunity* 2023;56:1631–48.
- Tichet M, Wulschleger S, Chryplewicz A, *et al.* Bispecific PD1-IL2v and anti-PD-L1 break tumor immunity resistance by enhancing stem-like tumor-reactive CD8+ T cells and reprogramming macrophages. *Immunity* 2023;56:162–79.
- Ye Q, Song D-G, Poussin M, *et al.* CD137 accurately identifies and enriches for naturally occurring tumor-reactive T cells in tumor. *Clin Cancer Res* 2014;20:44–55.
- Leem G, Park J, Jeon M, *et al.* 4-1BB co-stimulation further enhances anti-PD-1-mediated reinvigoration of exhausted CD39+ CD8 T cells from primary and metastatic sites of epithelial ovarian cancers. *J Immunother Cancer* 2020;8:e001650.
- Pérez-Ruiz E, Etcheberria I, Rodríguez-Ruiz ME, *et al.* Anti-CD137 and PD-1/PD-L1 Antibodies En Route toward Clinical Synergy. *Clin Cancer Res* 2017;23:526–8.
- Wei H, Zhao L, Li W, *et al.* Combinatorial PD-1 blockade and CD137 activation has therapeutic efficacy in murine cancer models and synergizes with cisplatin. *PLoS ONE* 2013;8:e84927.
- Woroniecka KI, Rhodin KE, Dechant C, *et al.* 4-1BB Agonism Averts TIL Exhaustion and Licenses PD-1 Blockade in Glioblastoma and Other Intracranial Cancers. *Clin Cancer Res* 2020;26:1349–58.
- Geuijen C, Tacke P, Wang L-C, *et al.* A human CD137xPD-L1 bispecific antibody promotes anti-tumor immunity via context-dependent T cell costimulation and checkpoint blockade. *Nat Commun* 2021;12:4445.
- Jeong S, Park E, Kim H-D, *et al.* Novel anti-4-1BBxPD-L1 bispecific antibody augments anti-tumor immunity through tumor-directed T-cell activation and checkpoint blockade. *J Immunother Cancer* 2021;9:e002428.
- Lakins MA, Koers A, Giambalvo R, *et al.* FS222, a CD137/PD-L1 Tetraivalent Bispecific Antibody, Exhibits Low Toxicity and Antitumor Activity in Colorectal Cancer Models. *Clin Cancer Res* 2020;26:4154–67.
- Muik A, Altintas I, Gieseke F, *et al.* An Fc-inert PD-L1x4-1BB bispecific antibody mediates potent anti-tumor immunity in mice by combining checkpoint inhibition and conditional 4-1BB co-stimulation. *Oncoimmunology* 2022;11:2030135.
- Muik A, Garraza E, Altintas I, *et al.* Preclinical Characterization and Phase I Trial Results of a Bispecific Antibody Targeting PD-L1 and 4-1BB (GEN1046) in Patients with Advanced Refractory Solid Tumors. *Cancer Discov* 2022;12:1248–65.
- Yuwen H, Wang H, Li T, *et al.* ATG-101 Is a Tetraivalent PD-L1x4-1BB Bispecific Antibody That Stimulates Antitumor Immunity through PD-L1 Blockade and PD-L1-Directed 4-1BB Activation. *Cancer Res* 2024;84:1680–98.
- Zhai T, Wang C, Xu Y, *et al.* Generation of a safe and efficacious llama single-domain antibody fragment (vHH) targeting the membrane-proximal region of 4-1BB for engineering therapeutic bispecific antibodies for cancer. *J Immunother Cancer* 2021;9:e002131.
- Bajaj G, Nazari F, Presler M, *et al.* 786 Dose selection for duobody®-pd-1x4-1bb (gen1046) using a semimechanistic pharmacokinetics/pharmacodynamics model that leverages preclinical and clinical data. *SITC 36th Anniversary Annual Meeting (SITC 2021) Abstracts* 2021.
- Cao Y, Balthasar JP, Jusko WJ. Second-generation minimal physiologically-based pharmacokinetic model for monoclonal antibodies. *J Pharmacokinet Pharmacodyn* 2013;40:597–607.
- Baxter LT, Zhu H, Mackensen DG, *et al.* Physiologically based pharmacokinetic model for specific and nonspecific monoclonal

- antibodies and fragments in normal tissues and human tumor xenografts in nude mice. *Cancer Res* 1994;54:1517–28.
- 31 Zalba S, Contreras-Sandoval AM, Martisova E, et al. Quantification of Pharmacokinetic Profiles of PD-1/PD-L1 Antibodies by Validated ELISAs. *Pharmaceutics* 2020;12:595.
 - 32 Zheng S, Wang W, Aldahdooh J, et al. SynergyFinder Plus: Toward Better Interpretation and Annotation of Drug Combination Screening Datasets. *Genomics Proteomics Bioinformatics* 2022;20:587–96.
 - 33 Jure-Kunkel M, Masters G, Girit E, et al. Synergy between chemotherapeutic agents and CTLA-4 blockade in preclinical tumor models. *Cancer Immunol Immunother* 2013;62:1533–45.
 - 34 Georgiev P, Muise ES, Linn DE, et al. Reverse Translating Molecular Determinants of Anti-Programmed Death 1 Immunotherapy Response in Mouse Syngeneic Tumor Models. *Mol Cancer Ther* 2022;21:427–39.
 - 35 Carretta M, Thorseth M-L, Schina A, et al. Dissecting tumor microenvironment heterogeneity in syngeneic mouse models: insights on cancer-associated fibroblast phenotypes shaped by infiltrating T cells. *Front Immunol* 2023;14:1320614.
 - 36 Lusheshi NM, Coates-Ulrichsen J, Harper J, et al. Transformation of the tumour microenvironment by a CD40 agonist antibody correlates with improved responses to PD-L1 blockade in a mouse orthotopic pancreatic tumour model. *Oncotarget* 2016;7:18508–20.
 - 37 Cao J, Chen S, An P, et al. Systematic pan-cancer analysis identifies DNASE2 as a potential prognostic marker and immunotherapeutic target for glioblastoma multiforme. *Genes Dis* 2025;12:101431.
 - 38 Dhir A, Dhir S, Borowski LS, et al. Mitochondrial double-stranded RNA triggers antiviral signalling in humans. *Nature New Biol* 2018;560:238–42.
 - 39 Jena KK, Mehto S, Nath P, et al. Autoimmunity gene IRGM suppresses cGAS-STING and RIG-I-MAVS signaling to control interferon response. *EMBO Rep* 2020;21:e50051.
 - 40 Lim J, Rodriguez R, Williams K, et al. The Exonuclease TREX1 Constitutes an Innate Immune Checkpoint Limiting cGAS-STING-Mediated Antitumor Immunity. *Cancer Immunol Res* 2024;12:663–72.
 - 41 Torres-Odio S, Lei Y, Gispert S, et al. Loss of Mitochondrial Protease CLPP Activates Type I IFN Responses through the Mitochondrial DNA-cGAS-STING Signaling Axis. *J Immunol* 2021;206:1890–900.
 - 42 He K, Barsoumian HB, Puebla-Osorio N, et al. Inhibition of STAT6 with Antisense Oligonucleotides Enhances the Systemic Antitumor Effects of Radiotherapy and Anti-PD-1 in Metastatic Non-Small Cell Lung Cancer. *Cancer Immunol Res* 2023;11:486–500.
 - 43 Lanahan SM, Wymann MP, Lucas CL. The role of PI3K γ in the immune system: new insights and translational implications. *Nat Rev Immunol* 2022;22:687–700.
 - 44 Jung I-Y, Narayan V, McDonald S, et al. BLIMP1 and NR4A3 transcription factors reciprocally regulate antitumor CAR T cell stemness and exhaustion. *Sci Transl Med* 2022;14:eabn7336.
 - 45 Zhao H, Liu Y, Wang L, et al. Genome-wide fitness gene identification reveals Roquin as a potent suppressor of CD8 T cell expansion and anti-tumor immunity. *Cell Rep* 2021;37:110083.
 - 46 Codarri Deak L, Nicolini V, Hashimoto M, et al. PD-1-cis IL-2R agonism yields better effectors from stem-like CD8⁺ T cells. *Nature New Biol* 2022;610:161–72.
 - 47 Hashimoto M, Araki K, Cardenas MA, et al. PD-1 combination therapy with IL-2 modifies CD8⁺ T cell exhaustion program. *Nature New Biol* 2022;610:173–81.
 - 48 Siddiqui I, Schaeuble K, Chennupati V, et al. Intratumoral Tcf1+PD-1+CD8⁺ T Cells with Stem-like Properties Promote Tumor Control in Response to Vaccination and Checkpoint Blockade Immunotherapy. *Immunity* 2019;50:195–211.
 - 49 Hudson WH, Gensheimer J, Hashimoto M, et al. Proliferating Transitory T Cells with an Effector-like Transcriptional Signature Emerge from PD-1⁺ Stem-like CD8⁺ T Cells during Chronic Infection. *Immunity* 2019;51:1043–58.
 - 50 Prokhnevska N, Cardenas MA, Valanparambil RM, et al. CD8⁺ T cell activation in cancer comprises an initial activation phase in lymph nodes followed by effector differentiation within the tumor. *Immunity* 2023;56:107–24.
 - 51 Sade-Feldman M, Yizhak K, Bjorgaard SL, et al. Defining T Cell States Associated with Response to Checkpoint Immunotherapy in Melanoma. *Cell* 2018;175:998–1013.
 - 52 Moynihan KD, Kumar MP, Sultan H, et al. IL2 Targeted to CD8⁺ T Cells Promotes Robust Effector T-cell Responses and Potent Antitumor Immunity. *Cancer Discov* 2024;14:1206–25.
 - 53 Barsoumian HB, Yolcu ES, Shirwan H. 4-1BB Signaling in Conventional T Cells Drives IL-2 Production That Overcomes CD4+CD25+FoxP3⁺ T Regulatory Cell Suppression. *PLoS ONE* 2016;11:e0153088.
 - 54 Oh HS, Choi BK, Kim YH, et al. 4-1BB Signaling Enhances Primary and Secondary Population Expansion of CD8⁺ T Cells by Maximizing Autocrine IL-2/IL-2 Receptor Signaling. *PLoS ONE* 2015;10:e0126765.
 - 55 Wu W, Chia T, Lu J, et al. IL-2R α -biased agonist enhances antitumor immunity by invigorating tumor-infiltrating CD25+CD8⁺ T cells. *Nat Cancer* 2023;4:1309–25.
 - 56 Silva R, Lopes MF, Travassos LH. Distinct T helper cell-mediated antitumor immunity: T helper 2 cells in focus. *Cancer Pathog Ther* 2023;1:76–86.
 - 57 Bai Z, Woodhouse S, Zhao Z, et al. Single-cell antigen-specific landscape of CAR T infusion product identifies determinants of CD19-positive relapse in patients with ALL. *Sci Adv* 2022;8:eabj2820.
 - 58 Feng B, Bai Z, Zhou X, et al. The type 2 cytokine Fc-IL-4 revitalizes exhausted CD8⁺ T cells against cancer. *Nature New Biol* 2024;634:712–20.
 - 59 McNally A, Hill GR, Sparwasser T, et al. CD4+CD25⁺ regulatory T cells control CD8⁺ T-cell effector differentiation by modulating IL-2 homeostasis. *Proc Natl Acad Sci U S A* 2011;108:7529–34.
 - 60 Curran MA, Kim M, Montalvo W, et al. Combination CTLA-4 blockade and 4-1BB activation enhances tumor rejection by increasing T-cell infiltration, proliferation, and cytokine production. *PLoS ONE* 2011;6:e19499.
 - 61 Palmeri JR, Lax BM, Peters JM, et al. CD8⁺ T cell priming that is required for curative intratumorally anchored anti-4-1BB immunotherapy is constrained by Tregs. *Nat Commun* 2024;15:1900.
 - 62 Dammeijer F, van Gulijk M, Mulder EE, et al. The PD-1/PD-L1-Checkpoint Restrains T cell Immunity in Tumor-Draining Lymph Nodes. *Cancer Cell* 2020;38:685–700.
 - 63 Tang H, Liang Y, Anders RA, et al. PD-L1 on host cells is essential for PD-L1 blockade-mediated tumor regression. *J Clin Invest* 2018;128:96061:580–8.
 - 64 Nagasaki J, Inozume T, Sax N, et al. PD-1 blockade therapy promotes infiltration of tumor-attacking exhausted T cell clonotypes. *Cell Rep* 2022;38:110331.
 - 65 Huang Q, Wu X, Wang Z, et al. The primordial differentiation of tumor-specific memory CD8⁺ T cells as bona fide responders to PD-1/PD-L1 blockade in draining lymph nodes. *Cell* 2022;185:4049–66.
 - 66 Rahim MK, Okholm TLH, Jones KB, et al. Dynamic CD8⁺ T cell responses to cancer immunotherapy in human regional lymph nodes are disrupted in metastatic lymph nodes. *Cell* 2023;186:1127–43.
 - 67 Yost KE, Satpathy AT, Wells DK, et al. Clonal replacement of tumor-specific T cells following PD-1 blockade. *Nat Med* 2019;25:1251–9.
 - 68 Jansen CS, Prokhnevska N, Master VA, et al. An intra-tumoral niche maintains and differentiates stem-like CD8 T cells. *Nature New Biol* 2019;576:465–70.
 - 69 Ziblat A, Horton BL, Higgs EF, et al. Batf3⁺ DCs and the 4-1BB/4-1BBL axis are required at the effector phase in the tumor microenvironment for PD-1/PD-L1 blockade efficacy. *Cell Rep* 2024;43:114141.
 - 70 Aerts J, Paz-Ares LG, Helissey C, et al. Acasunlimab (DuoBody-PD-L1x4-1BB) alone or in combination with pembrolizumab (pembro) in patients (pts) with previously treated metastatic non-small cell lung cancer (mNSCLC): Initial results of a randomized, open-label, phase 2 trial. *JCO* 2024;42:2533.